

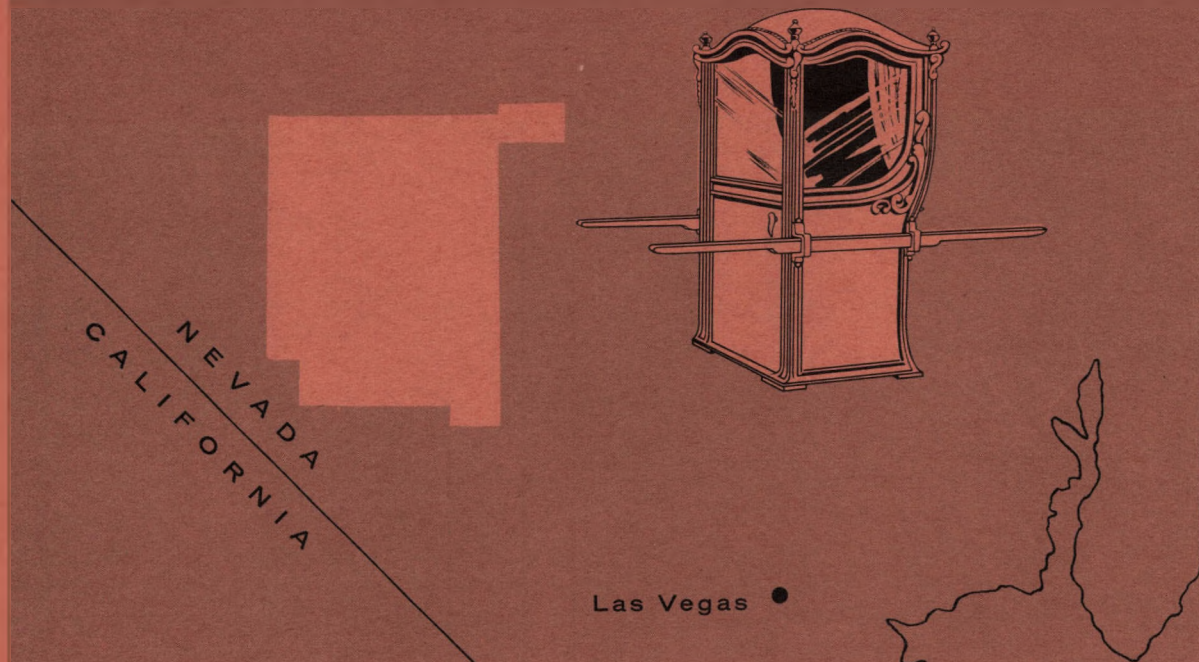
PNE-213F  
FINAL REPORT

Plowshare / peaceful uses for nuclear explosives

UNITED STATES ATOMIC ENERGY COMMISSION / PLOWSHARE PROGRAM

*project* SEDAN

NEVADA TEST SITE / JULY 6, 1962



**Seismic Effects from a High Yield Nuclear  
Cratering Experiment in Desert Alluvium**

W. V. Mickey

COAST AND GEODETIC SURVEY

ISSUED: APRIL 30, 1963

## LEGAL NOTICE

This report was prepared as an account of Government sponsored work. Neither the United States, nor the Commission, nor any person acting on behalf of the Commission:

- A. Makes any warranty or representation, expressed or implied, with respect to the accuracy, completeness, or usefulness of the information contained in this report, or that the use of any information, apparatus, method, or process disclosed in this report may not infringe privately owned rights; or
- B. Assumes any liabilities with respect to the use of, or for damages resulting from the use of any information, apparatus, method, or process disclosed in this report.

As used in the above, "person acting on behalf of the Commission" includes any employee or contractor of the Commission, or employee of such contractor, to the extent that such employee or contractor of the Commission, or employee of such contractor prepares, disseminates, or provides access to, any information pursuant to his employment or contract with the Commission, or his employment with such contractor.

This report has been reproduced directly from the best available copy.

Printed in USA. Price \$1.50. Available from the Office of Technical Services, Department of Commerce, Washington 25, D. C.

## **DISCLAIMER**

**This report was prepared as an account of work sponsored by an agency of the United States Government. Neither the United States Government nor any agency thereof, nor any of their employees, makes any warranty, express or implied, or assumes any legal liability or responsibility for the accuracy, completeness, or usefulness of any information, apparatus, product, or process disclosed, or represents that its use would not infringe privately owned rights. Reference herein to any specific commercial product, process, or service by trade name, trademark, manufacturer, or otherwise does not necessarily constitute or imply its endorsement, recommendation, or favoring by the United States Government or any agency thereof. The views and opinions of authors expressed herein do not necessarily state or reflect those of the United States Government or any agency thereof.**

---

## **DISCLAIMER**

**Portions of this document may be illegible in electronic image products. Images are produced from the best available original document.**

PROJECT SEDAN

PNE 213F

PROJECT 2.03

SEISMIC EFFECTS FROM A HIGH YIELD NUCLEAR CRATERING  
EXPERIMENT IN DESERT ALLUVIUM

W. V. Mickey  
Geophysicist

U. S. Department of Commerce  
Coast and Geodetic Survey  
Washington 25, D. C.

February 1963

## CONTENTS

	Page
ABSTRACT . . . . .	1
ACKNOWLEDGEMENTS . . . . .	2
CHAPTER 1 INTRODUCTION . . . . .	3
1.1 Objectives . . . . .	3
1.2 Background . . . . .	4
CHAPTER 2 PROCEDURE . . . . .	6
2.1 Seismograph Stations . . . . .	6
2.2 Instruments . . . . .	6
2.2.1 Project 1.4 Instruments . . . . .	6
2.2.1.1 Carder Displacement Meters . . . . .	7
2.2.1.2 Accelerometers . . . . .	8
2.2.2 Project 8.1 Instruments . . . . .	8
CHAPTER 3 RESULTS . . . . .	10
CHAPTER 4 DISCUSSION . . . . .	12
4.1 Maximum Signal Attenuation Characteristics . . . . .	12
4.2 Seismic Energy . . . . .	14
4.3 Travel Time and Depth Determinations . . . . .	19
4.4 Spectral Analysis . . . . .	20
CHAPTER 5 CONCLUSIONS AND RECOMMENDATIONS . . . . .	23
5.1 Conclusions . . . . .	23
5.2 Recommendations . . . . .	26
REFERENCES . . . . .	33
TABLES	
1.1 Event SEDAN DATA . . . . .	5
2.1 Station Participation . . . . .	27
2.2 Station Locations . . . . .	28
3.1 Event SEDAN Strong-Motion Seismic Data . . . . .	29
3.2 Event SEDAN Mobile Station Seismic Data . . . . .	31
3.3 Particle Velocities . . . . .	32
FIGURES	
2.1 Strong-motion seismograph station . . . . .	35
2.2 Response curves for a typical Carder Displacement Meter and an accelerometer . . . . .	36
2.3 Dynamic range of displacement meter . . . . .	37
2.4 Dynamic range of accelerometer . . . . .	38
2.5 System response for HTL, 14A, and 19L geophones . . . . .	39

## CONTENTS (con.)

	Page
<b>FIGURES (con.)</b>	
2.6 System response for Model 6102 seismometer . . . . .	40
2.7 Mobile station seismometer layout . . . . .	41
3.1 Observed particle accelerations and displacements from strong-motion stations. The solid line represents the prediction function . . . . .	42
3.2 Observed particle velocities and displacements from the intermediate range mobile seismograph stations . . . . .	43
3.3 SEDAN and seismograph station locations contoured from observed displacements . . . . .	44
3.4 SEDAN and seismograph station locations contoured from observed accelerations . . . . .	45
3.5 Surface earth motion versus yields for SCOOTER, DANNYBOY, and SEDAN . . . . .	46
3.6 Travel time-distance plot of maximum earth motion . . . . .	47
3.7 Travel time-distance plot of first arrivals of seismic energy . . . . .	48
3.8 Frequency versus amplitude from vertical component of displacement at Station 18 . . . . .	49
3.9 Frequency versus amplitude from radial component of displacement at Station 18 . . . . .	50
3.10 Frequency versus amplitude from transverse component of displacement at Station 18 . . . . .	51
3.11 Frequency versus amplitude from vertical component of displacement at Station 9-801 . . . . .	52
3.12 Frequency versus amplitude from radial component of displacement at Station 9-801 . . . . .	53
3.13 Frequency versus amplitude from transverse component of displacement at Station 9-801 . . . . .	54
3.14 Frequency versus amplitude for first 89 digital values of figure 3.11 representing real time of 1.44 to 6.33 seconds . . . . .	55
3.15 Frequency versus amplitude for digital values 90 through 234 of figure 3.11. This is a continuation of figure 3.14 representing real time interval of 6.33 through 14.39 seconds . . . . .	56
3.16 Frequency versus amplitude for digital values 1 through 89 and 90 through 234 of figure 3.12. This represents two real time segments of 1.22 to 6.11 seconds and 6.16 to 14.17 seconds . . . . .	57
3.17 Frequency versus amplitude for digital values 1 through 89 and 90 through 234 of figure 3.13. This represents two real time segments of 1.22 to 6.11 seconds and 6.16 to 14.17 seconds . . . . .	58

✓ (Supplied PNE-213 P.)

## ABSTRACT

SEDAN was a thermonuclear cratering experiment with a yield of about 100 kt detonated at a depth of 660 feet and resulting in a crater of maximum apparent depth of 635 feet and average apparent diameter of about 1200 feet. About 7.5 million cubic yards of earth and rock were displaced. Transitory earth particle motions were on an average twice as large from stations on deep alluvial deposits compared to those on shallow deposits at the same distance. Computed seismic energy was about  $2.45 \times 10^{18}$  ergs, equivalent to a local earthquake magnitude of 4.75. This indicates that .06 percent of the total source energy was converted to seismic energy. Frequency analysis revealed spectral peaks near 1 cps. 14 references. *Final*

#### ACKNOWLEDGEMENTS

Grateful acknowledgements are due personnel of numerous organizations such as Field Command DASA, AFTAC, and LRL. The success of the Project can be largely attributed to the work of the Special Projects Field Party personnel of the Coast and Geodetic Survey. T. R. Shugart is responsible for the spectral analysis section and the automatic data processing used to reduce the seismic data. Particular recognition is due the administrative supervision provided by Captains R. A. Earle and P. A. Weber and Mr. L. M. Murphy.

## CHAPTER 1

### INTRODUCTION

Project SEDAN was a cratering experiment in desert alluvium. A thermonuclear device was detonated at a depth of 635 feet in a 36 inch diameter cased hole which was backfilled with dry sand. The secondary explosion and flash occurred at approximately 3 seconds after zero when a 600 to 800 foot diameter dome of crater debris was at a height of 290 feet. The detonation displaced about 7.5 million cubic yards of earth (Kelly, 1962).

The Coast and Geodetic Survey monitored surface earth motions from the DANNYBOY nuclear cratering experiment in basalt and the desert alluvium high-explosive experiment SCOOTER (Mickey, 1961; Mickey and Pearce, 1962). SEDAN was in the same general area and medium as SCOOTER.

The purposes of the experiment were to derive a scaling function in the 100 to 200 kt range at a greater than optimum depth of burial and to determine the possibility of extrapolating the crater prediction functions to the megaton range.

#### 1.1 OBJECTIVES

The Coast and Geodetic Survey measured transitory earth particle surface motions in terms of displacements, velocities, and accelerations in the distance range where the normal elastic response is applicable.

The objectives of the Survey's seismic measurement program were:

1. To determine the magnitude and attenuation with distance of

the peak earth particle displacements, velocities, and accelerations; and

2. To compare results obtained from studies of previous underground detonations and natural earthquake phenomena for the purpose of improving empirical scaling formulas for earth particle motion predictions.

## 1.2 BACKGROUND

Scaling functions were developed by the Coast and Geodetic Survey for nuclear events at the Nevada Test Site of the Atomic Energy Commission during the PLUMBOB and HARDTACK II Series (Carder, et. al., 1958 and 1961). The distance range from the source to the detector varied from less than 1 to 1,000 km. In a later report, (Mickey et. al., 1962), scaling functions were derived for NTS events of the NOUGAT and STORAX Series as recorded on the strong-motion seismographs within a distance range of 0.4 to 21.3 km. During the same series, scaling functions were computed with data from Benioff Variable Reluctance seismometers for earth particle displacements and earth particle velocities from moving coil geophones.

A summary of the scaling functions for the parameters measured are:

U. S. Coast and Geodetic Survey Strong Motion Seismographs

$$a = .0041W^{0.54}R^{-1.4} \quad 0.4 \text{ to } 21.3 \text{ km}$$

$$d = .0027W^{0.8}R^{-1.2} \quad 0.4 \text{ to } 21.3 \text{ km}$$

Portable Benioff Seismometers

$$d = .000165W^{0.8}R^{-1.2} \quad 18 \text{ to } 350 \text{ km}$$

### Moving Coil Geophones

$$v = .0144W^{0.67}R^{-1.5} \quad 18 \text{ to } 350 \text{ km}$$

Where:  $d$ ,  $v$ , and  $a$  = peak earth particle displacements, velocities, and accelerations in cm, cm/sec and gravity units.

$W$  = equivalent TNT yield in tons.

$R$  = source to detector distance in km.

Based upon the SCOOTER measurements with the strong-motion instruments, the ratio of anticipated (based upon the above formula) to measured displacements was 0.62 and for accelerations was 1.46. This indicates that displacements were larger than anticipated and that the accelerations were less.

The ratios for the DANNYBOY Event were 1.3 for displacements and 2.2 for accelerations. The yields were nearly the same, (0.5 kt high explosive for SCOOTER and 0.42 nuclear kt for DANNYBOY), but the source media and energy source differed.

Drill holes in the area of SEDAN indicated that the alluvium was about 370 meters thick and overlies a weakly cemented sandy tuff, gradually changing to tuff similar to that found in the Rainier Mesa. Table 1.1 lists the pertinent data for SEDAN.

Table 1.1.--Event SEDAN Data

Date and Time GMT	Coordinates		Elevation Surface and W.P.	Probable Yield
	Nevada Control Zone Grid	Geographic	ft	kt
July 6, 1962	N 884000	N $37^{\circ}10'37''$	4317	<u>100 <math>\pm</math> 15</u>
17:00:00.147	E 681000	W $116^{\circ}02'43''$	3657	

## CHAPTER 2

### PROCEDURE

#### 2.1 SEISMOGRAPH STATIONS

To provide adequate seismic instrumentation for the large scale cratering experiment, eight of the strong-motion seismograph stations were located in concrete bunkers and installations which had been constructed for purposes other than seismograph stations. Three of the stations which were out of the debris fallout range were located in seismograph shelters at distances of 7.02, 10.88, and 13.53 km from ground zero.

Three of the six mobile seismograph stations were located on a radial line northeast of ground zero at approximately 50 km intervals beginning at 150 km. One station was operated at Tryon, Oklahoma. Two stations were operated near Suffield, Alberta, Canada.

Tables 2.1 and 2.2 list the seismograph location data. The station locations are shown in figure 2.1 for Project 1.4.

#### 2.2 INSTRUMENTS

The seismographs operated for the SEDAN Event were divided into two projects, 1.4 and 8.1. Project 1.4 instruments were strong-motion seismographs (eleven stations) operating in the distance range of 1.1 to 27.0 km. Project 8.1 consisted of instruments used with the mobile seismograph stations in the distance range of 151 to 1712 km.

2.2.1 Project 1.4 Instruments. Project 1.4 stations were instrumented with the standard strong-motion accelerograph used by the

Coast and Geodetic Survey for earthquake monitoring. Each seismograph was anchored to a concrete pad which was bonded to the ground surface. A small house was constructed over each station to provide shelter and darkroom facilities for changing and loading the photographic paper.

Each seismograph consisted of a camera, dynamic elements, timing devices, and remote control circuitry. Torsional or compound pendulums comprised the dynamic elements and their motions, relative to the earth, were recorded on photographic paper through a system of optical levers. Calibration of the individual instruments was by tilt and free period tests prior to installation and by period and damping tests after installation. Internal timing was imposed on each seismogram with back-up time control (1 pulse/sec) simultaneously supplied by EG&G to Station 18 and thence wire-linked to each station.

The instruments were actuated by a -2 or -1 second closure of EG&G relays through a land line signal or an EG&G "tone radio receiver." Closure of an EG&G zero time relay was used to reference firing time on each record. Each recorder was stopped by the opening of a mechanical circuit breaker after approximately two minutes operation. Recording paper speeds were 10 cm/sec.

2.2.1.1 Carder Displacement Meters (CDM). The horizontal Carder Displacement Meter consisted of a compound pendulum which recorded the horizontal components of earth motion by means of optical-mechanical recording on photographic paper. The natural periods varied from less than 1 to over 3 seconds, depending upon the magnification desired. The magnification ranged from less than 1 to over 8. Vertical displacement

components of earth motion were recorded by dynamic components consisting of small disks mounted on pivot and jewel spindles. The effective pendulum length was governed by offset weights on the rim of the disks with coiled springs supplying the balance and restoring forces. Magnification for the vertical displacement meters was near unity with normal instrument periods of about 2.5 sec.

Figure 2.2 shows response curves of a typical Carder Displacement Meter and an accelerometer. Figure 2.3 gives the dynamic range of the displacement meter.

2.2.1.2 Accelerometers (ACCEL). The horizontal accelerometer was essentially a torsion seismometer with an inertia mass suspended eccentrically on a vertical fiber so that it virtually acted as a horizontal pendulum, the period of which was controlled by the torsional reaction in the fiber and a small gravity component. The vertical seismometer had a horizontal fiber element. Damping was provided for both vertical and horizontal components by permanent magnets. The seismic information was recorded on photographic paper by an optical-mechanical system. Instrumental periods of 0.03 to 0.4 sec were used with static magnification of about 120, sensitivities of 2.3 to 70 cm/g, and damping about 60 percent critical. Figure 2.4 is an example of the dynamic range of the accelerometer.

2.2.2 Project 8.1 Instruments. Stations IR17, IR18, IR19, LR1 and LR2 had three components of 14A, HTL and 19L geophones (see figure 2.5). Three components of the miniature Benioff Variable Reluctance (BVR)

seismometers were also operated (see figure 2.6).

The 19L, 14A, and HTL geophones consisted of a coil moving in the field of a permanent magnet generating voltage sufficient to deflect a sensitive galvanometer. The seismic energy was electronically amplified by NGC-25-C amplifiers with a flat response from 2 to 18 cps.

The natural period of the 19L and HTL geophones was 2 cps with damping 0.67 critical. The 14A geophones had a natural period of about 8.5 cps and damping about 0.65 critical. The seismic energy was converted to analog form by a light beam reflected from the galvanometer to an oscilloscope. Magnification was controlled and predetermined by the yield and detector to source distances. The geophone data were recorded on photographic paper and on a 3170 Minneapolis-Honeywell magnetic tape recording system.

The BVR seismometers were operated with free periods of about 1 cps and damping about 0.65 critical. The outputs drove 5 cps galvanometers in a four-channel film recorder with the fourth used to record WWV timing signals and to program time marks every 10 seconds except at the minutes. This reference signal was recorded on all channels for time controls. The Benioff data were recorded on 35 mm film by a Mark I film recorder and on the magnetic tape.

The three-component patterns of 14A, HTL, and BVR seismometers were located near the recording trailer with a linear array of three vertical 19L geophones located at 1000 foot intervals on a radial line from NTS (see figure 2.7).

The Oklahoma station had three components of the BVR seismometers recording on 35 mm film and magnetic tape.

## CHAPTER 3

### RESULTS

Tables 3.1 and 3.2 list the recorded transitory earth particle motion in terms of displacements, velocities, and accelerations. The values are obtained by scaling the largest peak excursions on the seismograms and applying the appropriate instrumental response to arrive at earth motion.

Figures 3.1 and 3.2 are graphical plots of the seismic data with the prediction function plotted for comparison with the observed values.

Figures 3.3 and 3.4 show the recorded displacements and acceleration for the eleven strong-motion stations. The contours shown on figure 3.3 are at 10 km based on an attenuation with distance function of  $R^{-1.2}$ . The contour interval for figure 3.4 is at 5 km intervals based on an attenuation with distance function of  $R^{-1.4}$ . Except for contour values of less than 0.28, the interval is 10 km.

Figure 3.5 is a graph showing the earth motion versus yield for DANNYBOY, SCOOTER, and SEDAN.

Figure 3.6 is a plot of the travel time of the pulse corresponding to the maximum motion. The stations with the longer time of arrivals are those stations located on the down-thrown side of the YUCCA fault in the deep alluvial fill. The stations with the shorter travel times are those on the west or up-thrown side of YUCCA fault which has a much shallower deposit of alluvium.

A travel time versus distance plot is shown in figure 3.7. Here again the effect of the deep alluvium is apparent with the longer travel time associated with the lower velocity alluvium.

Fourier integral spectra analysis was made on the displacement seismograms from Stations 18 and 9-801. The spectra plots are shown in figures 3.8 through 3.17.

## CHAPTER 4

### DISCUSSION

#### 4.1 MAXIMUM SIGNAL ATTENUATION CHARACTERISTICS

Earth motion prediction functions have been developed (a posteriori) for a large number of detonations at the Nevada Test Site. Applying these functions to the strong-motion seismic data from SCOOTER with twelve observation points for both displacements and accelerations, the anticipated accelerations, on an average, were 1.46 times larger than the measured values. The anticipated displacements were 0.62 times as large as measured.

For the DANNYBOY Event the ratio of anticipated to measured motion was 2.2 for acceleration and 1.3 for displacement from nine observation points.

SCOOTER was a 0.5 kt high-explosive detonation in desert alluvium with the recording stations on alluvium. DANNYBOY was a  $0.42 \pm .04$  nuclear detonation in a basalt flow with the recording stations located on the basalt.

Comparison of recent contained nuclear detonations in alluvium, salt, tuff, and granite has shown that the conversion of source to seismic energy is the least efficient in alluvium. It has been shown that maximum earth motion is recorded at stations on deep alluvial deposits; therefore, the decrease of seismic source energy in alluvium coupled with the increase of earth motion on alluvium as compared to an increase of seismic source energy in basalt with a decrease of earth

motion in competent rock makes feasible a comparison of SCOOTER and DANNYBOY.

Figure 3.1 shows the measured values of peak displacement and acceleration with a comparison to the predicted values. From this figure it can be seen that the stations located on the east side of YUCCA fault recorded larger earth motions than those on the west side. Asymmetric source conditions are questionable as a cause since the condition exists at Stations 24 and 1-300 which were the same distances from the source and on the down- and up-thrown sides of the fault, respectively, but with a difference in azimuth of only 24 degrees.

Figure 3.2 shows the seismic data from the mobile stations in the distance range of 151 to 1712 km. The signal attenuation with distance for the displacements are closer to the inverse square law based on the information at Stations LR1, LR2, and Oklahoma. The 1.2 exponent for distance was developed from data which were less than 350 km. For Stations IR17, 18, and 19 the deviation of the observed to predicted displacements was the same order of magnitude as the strong-motion data.

The particle velocities from Stations IR17, 18, and 19 differ from the other seismic data with greater than predicted values recorded at Station IR17 with distance exponential of 3.0 indicated. The field data and operational diary were checked to see if the anomaly was instrumental. The data were substantiated. To further check the condition, particle velocities were calculated from the Benioff displacement data assuming simple harmonic motion. The computed velocities were near those recorded. The high values could be explained by the maximum motion being

transmitted at higher than normal frequencies but this hypothesis is negated by the conformity of the strong-motion accelerations and displacements.

Figures 3.3 and 3.4 show the effect of the propagation path on the data more clearly. The contour values are selected to fit the attenuation data arrived at by earlier detonations. If the data were compatible with the scaling functions and the energy propagation were symmetrical, the contours would be arcs of concentric circles at equidistance spacing. The signal attenuation is definitely greater for the stations on the shallower alluvial deposits to the west of YUCCA fault.

Another comparison can be made by observing the ratio of the anticipated motion to the recorded motion from stations on each side of the fault.

#### Ratios of Anticipated Motion to Recorded Motion

Acceleration	n*	Displacement	n*
17.3	16	9.5	14 West Side
7.9	12	4.9	11 East Side
13.3	28	7.5	25 All Stations

\*n is the number of observations.

#### 4.2 SEISMIC ENERGY

It is normal to expect less source seismic energy from a cratering shot as compared to a contained detonation of equivalent yield; however, since SCOOTER and DANNYBOY produced earth motion in agreement with functions derived from contained detonations, it was thought there could be agreement for the predicted earth motions from SEDAN. Considering the eleven SEDAN stations, the ratios of predicted to measured varied from 4.9 to 17.3 for accelerations and displacements.

Stations were selected which were approximately the same distance from the three events SCOOTER, DANNYBOY, and SEDAN. The following stations and distances were selected to investigate an empirical yield exponent to explain the deviation from predictions.

Group	Station	Distance km	Event
1	1	1.52	SCOOTER
1	18-2	1.22	DANNYBOY
1	7.2a2	1.13	SEDAN
2	2	2.67	SCOOTER
2	18-3	2.13	DANNYBOY
2	18	2.33	SEDAN
3	3	3.55	SCOOTER
3	9-801	3.84	SEDAN

Figure 3.5 is an amplitude versus yield plot used to arrive at the yield scaling exponent between the SCOOTER and DANNYBOY events relative to SEDAN. The resulting exponents are 0.27 for acceleration and 0.38 for displacement. This compares to the exponents derived from earlier data of 0.54 and 0.8. It will be noted that the difference is near a factor of 2.

Since the earth motion differed from equidistant stations on deep and shallow alluvium the arrival times of the maximum motion were also studied. Figure 3.6 is a plot of the travel time measured from zero time of detonation versus distance. The stations on the thick alluvial section recorded much longer times. The approximate velocity of the pulse registering the largest motion on the east side of YUCCA fault was 415 meters per second. The velocities on the west side seemed to increase with distance from ground zero.

There is much data in the literature on seismology concerning the magnitude and energy calculations of earthquakes (Gutenberg and Richter, 1956; Richter, 1958). Derivation of seismic energy from an explosive source has a more restricted bibliographical list. One approach is to relate seismic energy from an explosion to earthquake seismic energy and magnitudes. Using techniques for calculating source seismic energy for an explosion from the seismogram requires that various assumptions be made (Berg, et. al., 1961; Carder, et. al., 1958, 1961, 1962; and Howell and Budenstein, 1955).

Assumptions have to be made of the propagation characteristics, energy distribution or partitioning, and the properties of numerous other parameters which are not measurable within the limits of the present observations.

Based upon the thesis that the wave fronts are hemispherical, that the surface measurements are twice those within the earth, and that the measured phase represents one-fourth of the total seismic energy, the following formula could apply for transitory earth particle displacements:

$$E = \rho \pi^3 R^2 f d^2 V Q 10^{2kR}$$

Where:

$E$  = total source seismic energy in ergs

$\rho$  = density, 2.2 gm/cm<sup>3</sup>

$f$  = frequency

$V$  = propagation velocity, cm/sec

d = transitory earth particle displacement, cm

Q = factor for energy loss at seismic boundaries and assumed unity for the present example

k = absorption coefficient/km with 0.013 assumed

R = distance from source to detector, cm

Using the seismic data from eleven strong-motion stations gives the following energy values:

STATION	ENERGY $10^{18}$ ergs	MAGNITUDE $M_L$
7.2a2	1.40	4.60
18	0.652	4.41
9-801	4.40	4.90
2-300	0.412	4.29
27	5.40	4.96
4-480	2.38	4.74
4-330	0.452	4.31
26	4.75	4.92
24	6.05	4.98
1-300	.342	4.24
400	.728	4.44
AVERAGES	E2.45	$M_L$ 4.62

If a relationship exists between the energy from an earthquake and a point source event, the formula reported by Richter (1958), for local earthquakes would give an equivalent magnitude.

$$\log E = 9.9 + 1.9 M_L - 0.024 M_L^2$$

Solving for  $M_L$  with the average energy from the eleven stations of

$2.45 \times 10^{18}$  gives a local magnitude of 4.75. Converting this to a unified magnitude for comparison to the teleseismic observations gives  $m$  of 5.27 using the equation

$$m = 1.7 + 0.8 M_L - 0.01 M_L^2.$$

Converting back to energy using the equation presented by Richter (1958),

$$\log E = 5.8 + 2.4m$$

gives an energy value of  $10^{18.45}$  or  $2.82 \times 10^{18}$  ergs which is close to the  $2.45 \times 10^{18}$  as calculated.

The averages of the energy and magnitude calculations for the eleven stations illustrate a problem inherent in the accepted procedure of reporting an "average unified magnitude." Since magnitude is an exponential function and energy is linear, it seems more realistic to base average magnitude on average energy. With a magnitude assigned each station the average is 4.62 in contrast to 4.75 based on energy averages. This deviation is not great but could become a problem when larger variations are used for averaging.

The estimated seismic energy of SEDAN was .06 percent of the total energy based upon the computed average seismic energies for the eleven stations.

Energy calculations were applied to the SCOOTER and DANNYBOY strong-motion seismic data to investigate the comparative seismic source energy from a high-explosive and a nuclear detonation. Other observers (Pasechnik, et. al., 1960) have estimated that nuclear detonations produce one-fourth to one-half the seismic energy of

high-explosive cratering detonations. The two events were nearly the same equivalent yield detonated at about the same scaled depth but differed in source media and recording site conditions.

The average source seismic energy calculated for SCOOTER was  $1.68 \times 10^{17}$  ergs and for DANNYBOY was  $3.70 \times 10^{16}$  ergs with four data points used for SCOOTER and three data points for DANNYBOY. Since the yield differed, the seismic efficiency was computed for each event assuming that 1 kt of TNT equivalent is defined as the prompt release of  $10^{12}$  calories of energy or  $4.2 \times 10^{19}$  ergs. The seismic energy was 0.8 percent for SCOOTER and 0.21 percent for DANNYBOY of the total source yield. This would indicate that for the  $\frac{1}{2}$  kt range the nuclear event produced less seismic energy than a high-explosive shot by a factor of about 0.26 for the conditions existing for SCOOTER and DANNYBOY.

#### 4.3 TRAVEL TIME AND DEPTH DETERMINATIONS

Figure 3.7 shows the travel times for the first discernible trace motion at the nine strong-motion stations where there was adequate time control.

The strong-motion instruments of the 1.4 Project were not designed to record first motion at all distances from a source. If emphasis were on the first motion at more distant stations, the maximum trace deflection would be off the seismogram. An attempt was made to pick the first motion at all stations. The data scatter at the distant stations is indicative of the quality of the first break for arrival times.

The travel times were corrected to a datum plane of 1 km for depth of burst and station elevation. The near surface velocity of 1.5 km/sec was assumed since there was no travel time control at distances less than 1 km. The travel times for the stations on the east or down-thrown side of YUCCA fault indicated a depth of near 335 meters or 1100 feet. The four stations on the west side indicated a depth of 134 km or 440 feet which would result in a throw or fault displacement of about 201 meters or 660 feet.

#### 4.4 SPECTRAL ANALYSIS

Figures 3.8 through 3.17 are spectral plots from Stations 18 and 9-801 using a Fourier integral code on an IBM 1620 digital computer.

The earth motion from SEDAN as recorded on the strong-motion stations differed from the contained detonations in alluvium with the horizontal component recording much larger displacements than the vertical. A comparison of the ratios of horizontal to vertical motion is as follows for the three cratering experiments:

Event	Acceleration				Displacement			
	R/V	n	T/V	n	R/V	n	T/V	n
SCOOTER	1.2	4	1.2	4	1.1	4	1.4	4
DANNYBOY	2.0	3	1.2	3	0.9	3	0.3	3
SEDAN	1.4	9	1.7	9	5.0	6	5.3	6

n is number of observations.

R/V and T/V are ratios of radial and transverse motion to vertical.

Figures 3.8, 3.9, and 3.10 are Fourier plots of the vertical, radial, and transverse components of displacement for Station 18 at 2.33 km. The maximum amplitudes occur at about 0.7 cps. The Bensen-Lehner Osker Model K reader sensitivity for the digitized data was ten reader units/mm. The maximum motions on the original records were 7, 18, and 13 mm for the vertical, radial, and transverse. Prominent secondary spikes occur at 1 and 1.3 cps on the vertical, 1.2 on the radial, and 1.4 on the transverse.

The displacement seismograms for Station 9-801 were also digitized and processed by the same methods used for Station 18 with the results shown in figures 3.11, 3.12, and 3.13. In contrast to Station 18, which was on the up-thrown side of YUCCA fault, Station 9-801 was on the down-thrown side. The reader sensitivity was the same as for Station 18, but the maximum trace motion on the seismogram was 2, 20, and 20 mm. Figure 3.11 is an example of Fourier analysis of marginal data. The high, narrow spectral peaks over a wide band are not considered valid but are presented to show the results of analyzing a seismogram with trace motions too small. Plots 3.12 and 3.13 differ from the same components of Station 18 by the narrow spectra bands above 1 cps.

While figure 3.11 is of little value for valid spectral analysis, the data are in a form for determining at what real time on the seismogram that the peaks occurred. A Fourier integral analysis was applied to the first 89 digital values covering a time of 1.44 to 6.33 seconds.

The same method was used for digital values 90 through 14.39 seconds. The results are shown in figure 3.14 and 3.15. Spectral peak "C" was prominent in the early part of the record with peaks "A" and "B" in the second part.

The same methods were used to process the data for the horizontal components of Station 9-801. The overall Fourier results are shown in figures 3.13 and 3.14 with the two segments shown in figures 3.16 and 3.17. It is apparent from both figures 3.16 and 3.17 that the high-frequency perturbations of the Fourier amplitudes are characteristic of the early part of the record. The segment from 6.16 to 14.17 seconds for both radial and horizontal have very little spectral amplitude changes.

## CHAPTER 5

### CONCLUSIONS AND RECOMMENDATIONS

#### 5.1 CONCLUSIONS

The anticipated accelerations were 7.9 to 17.3 times larger than recorded and the anticipated displacements were 4.9 to 9.5 times larger than recorded. In all cases the recorded values were closer to predicted on the deep alluvial fill on the east side of YUCCA fault.

Stations equidistant from the source were selected for SCOOTER, DANNYBOY, and SEDAN to determine an approximate yield exponent for scaling from the smaller yields to SEDAN. If it can be assumed that a power function defines the scale relationship, a yield exponent for accelerations of 0.27 and for displacements of 0.38 is indicated. This compares with 0.54 and 0.8 exponents derived from earlier data.

The arrival times for the maximum motion were consistently longer for the stations in deep alluvium.

The calculated seismic energy was  $2.45 \times 10^{18}$  ergs from the data of the eleven strong-motion stations. This would imply that .06 percent of the total energy release was converted to seismic energy. An earthquake magnitude of 4.75 was indicated from accepted methods of relating energy to local earthquakes. Converting local magnitudes to teleseismic magnitude gives 5.27.

For one not versed in the terminology of magnitude and seismic energy, reference to intensity has more meaning. Intensity refers to the degree of shaking at a specific place, i.e., it describes the effect

of an earthquake. Magnitude refers to the total energy release at the source. The Modified Mercalli Intensity Scale ranges from MM-I to MM-XII. Richter (1958) defines these two intensities as follows:

- MM-I. Not felt. Marginal and long period effects of large earthquakes.
- MM-XII. Damage nearly total. Large rock masses displaced. Lines of sight and level distorted. Objects thrown into air.

There have been numerous attempts at relating intensity to measurable ground motion. Richter (1958) and Hershberger (1956) discuss the problems encountered in defining intensity in quantitative physical terms. One relationship is as follows:

$$\log a = .33(I) - 0.5$$

Where:

$a$  = acceleration in  $\text{cm/sec}^2$ .

(I) = the MM intensity.

Using this equation for the maximum acceleration at Station 7.2a2, which was 1.13 km from SEDAN, one arrives at an intensity of MM-IX which is defined as:

General panic. Masonry D destroyed; masonry C heavily damaged, sometimes with complete collapse; masonry B seriously damaged. (General damage to foundations). Frame structures, if not bolted, shifted off foundations. Frames rocked. Serious damage to reservoirs. Underground pipes broken. Conspicuous cracks in ground. In alluviated areas, sand and mud ejected, earthquake fountains, sand craters.

Masonry A, B, C, and D are defined as follows (Richter, 1958):

Masonry A. Good workmanship, mortar, and design; reinforced, especially laterally, and bound together by using steel, concrete, etc.; designed to resist lateral forces.

Masonry B. Good workmanship and mortar; reinforced but not designed in detail to resist lateral forces.

Masonry C. Ordinary workmanship and mortar; no extreme weaknesses like failing to tie in at corners, but neither reinforced nor designed against horizontal forces.

Masonry D. Weak materials, such as adobe; poor mortar; low standards of workmanship; weak horizontally.

There was no report of damage to the blast-resistant bunker which housed Station 7.2a2; however, the maximum recorded displacement was 4.25 cm.

Station 6-400 was 27.21 km from SEDAN and located near CP1. The intensity-acceleration formula for this station gave the following:

MM-II. Felt by persons at rest, on upper floors, or favorably placed.

The modified intensity formula suggested by Hershberger (1956) which states

$$\log a = .43(I) - 0.9$$

gives MM-VIII and MM-II for the two stations.

Travel times at stations on the east and west side of YUCCA fault indicated depths of 335 and 134 meters, resulting in a down-to-the-east throw of 201 meters.

Fourier spectral analysis for two stations were characterized by peaks near 1 cps.

## 5.2 RECOMMENDATIONS

Azimuthal energy propagation effects were noted with stations on both sides of YUCCA fault. It is suggested that for future experiments, stations be located on similar geologic formations on each side of the fault such as the Rainier Mesa member of the Piapi Canyon formation.

Intensity and magnitude scales have been developed for earthquakes. In anticipation of the large scale cratering applications of nuclear detonations, it seems that an intensity scale would be appropriate for damage criteria.

Table 2.1.--Station Participation

Station and Foundation	Nevada Central Zone Grid Coordinates	Station Elevation ft
1-300 Alluvium	N 839048 E 667620	4193
2-300 Alluvium	N 870102 E 663008	4405
4-480 Alluvium	N 854035 E 667420	4251
7.2a2 Alluvium	N 881276 E 678576	4284
9-801 Alluvium	N 871570 E 683029	4241
18 Alluvium	N 881442 E 673839	4381
24 Alluvium	N 839966 E 686698	4050
26 Alluvium	N 849054 E 688247	4175
27 Alluvium	N 861152 E 683865	4233
6-400 Dolomite	N 794766 E 678634	4215
4-330 Alluvium	N 854035 E 666517	4251

Table 2.2.--Station Locations

Station	Political Location	Geodetic Coordinates			Geographic Elevation
		o	'	"	ft
IR17	Lincoln County, Nevada	N 37 42 00	W 114 28 50		5100
IR18	Iron County, Utah	N 37 58 32	W 113 44 40		5500
IR19	Iron County, Utah	N 38 01 00	W 112 59 04		6100
IR Okla	Lincoln County, Oklahoma	N 35 52.0	W 96 57.5		800
LR1	Near Suffield, Alberta	N 50 29.12	W 112 23.18		2500
LR2	Near Suffield, Alberta	N 50 29.12	W 112 40.91		2900

Table 3.1.--Event SEDAN Strong-Motion Seismic Data

Station and Slant Distance from Working Point	Instrument and Component		Maximum Acceleration	Maximum Transient Displacement	Period	Travel Time
			$10^{-2} g$	$10^{-1} \text{cm}$	sec	sec
Station 7.2a2 1.127 km	ACCEL	V	11.3		0.29	0.57
		R	15.1		0.23	
		T	37.5		0.21	
	CDM	V		Not installed		
		R		42.5	1.50	
		T		16.9	1.49	
Station 18 2.328 km	ACCEL	V	Drifted off before event			
		R	11.5		0.30	1.04
		T	Negligible motion			
	CDM	V		2.34	1.13	
		R		12.2	1.07	
		T		10.7	1.31	
Station 9-801 3.843 km	CDM	V		4.57	0.58	
		R		19.4	1.28	
		T		13.4	1.51	1.22
Station 2-300 6.933 km	ACCEL	V	.583		0.24	
		R	.814		0.29	
		T	1.33		0.28	1.51
	CDM	V		.410	0.29	
		R		2.55	1.60	
		T		3.55	0.22	
Station 27 7.021 km	ACCEL	V	1.61		0.36	1.78
		R	2.74		0.63	
		T	2.16		0.87	
	CDM	V		.160	0.26	
		R		8.22	1.41	
		T		11.4	1.42	
Station 4-480 9.889 km	ACCEL	V	1.08		0.25	2.50
		R	1.49		0.60	
		T	1.65		0.50	
	CDM	V		Negligible motion		
		R		3.65	1.12	
		T		3.16	1.77	

Table 3.1.--Event SEDAN Strong-Motion Seismic Data (con.)

Station and Slant Distance from Working Point	Instrument and Component	Maximum Acceleration	Maximum Transient Displacement	Period	Travel Time
Station 4-330 10.146 km	ACCEL	$10^{-2}g$	$10^{-1}cm$	sec	sec
		V .873		0.31	No zero
		R 1.22		0.25	signal
	CDM	T 1.09		0.35	
		V	1.22	0.83	
		R	1.67	1.01	
		T	1.18	1.83	
	ACCEL	.756		1.00	2.33
		R .980		0.36	
		T .141		0.41	
Station 26 10.879 km	CDM	V	Negligible motion		
		R	5.16	1.55	
		T	6.78	1.49	
	ACCEL	.905		0.47	2.87
		R 1.06		1.05	
		T 1.24		0.55	
		CDM V	.527	0.41	
		R	4.00	1.45	
		T	4.70	1.48	
Station 24 13.534 km	ACCEL	.350		0.25	2.76
		R .530		0.43	
		T .381		0.38	
	CDM	V	.180	0.47	
		R	1.08	1.82	
		T	1.05	1.99	
Station 1-300 14.296 km	ACCEL	.090		0.30	No zero
		R .098		1.09	signal
		T .0805		1.22	
	CDM	V	Negligible motion		
		R	.494	1.83	
		T	.419	1.81	

ACCEL, CDM = Accelerations and displacements as recorded from the accelerometers and Carder Displacement Meters described in the text.

V, R, T = Vertical, radial, and transverse components of ground motion.

Table 3.2.--Event SEDAN Mobile Station Seismic Data

Station and Distance from Ground Zero	Com-ponent	First Motion Travel Time	P Phase			S Phase			Remarks
			Maximum Displace-ment	Period of Maximum Displace-ment	Maximum Displace-ment	Period of Maximum Displace-ment			
Okla 1712 km	V	3'40"?	$10^{-5}$ cm	?	-	$10^{-5}$ cm	.36	2.3	-
	T			?	-		.56	1.9	-
	R			?	-		.26	1.6	-
LR1 1906 km	V	3'15.9"		.30	1.3		.45	1.9	First motion up.
	T			.46	2.3		.62	1.8	
	R			?	-		1.9	1.8	High background.
LR2 1501 km	V	?		.27	1.4		1.0	2.2	Timing system failed; First motion up.
	T			?	-		.85	1.8	High background.
	R			?	-		.67	1.7	" "
IR17 151.1 km	V		13	0.26		5.4		0.44	First motion up.
	T	25.8"	8.0	0.26		22		0.61	
	R		9.8	0.35		21		0.69	
IR18 221.7 km	V	36.8"	4.9	0.39		16		0.71	
	T		8.6	0.53		47		0.79	
	R		6.0	0.53		30		0.79	
IR19 285.9 km	V		1.2	0.45		2.0		0.45	
	T	43.7"	1.2	0.45		7.4		0.58	
	R		2.0	0.31		1.1		0.68	

Table 3.3.--Particle Velocities

Station and Distance from GZ	Seismometer and Component	Particle Velocity	Period	First Arrival Travel Time
		$10^{-3}$ cm/sec	sec	sec
IR17 151.1 km	14A V	-	-	
	T	-	-	
	R	-	-	
	HTL V	22.7	0.24	25.6
	T	7.58	0.24	
	R	6.83	0.30	
	19L V	47.8	0.24	
	V	58.8	0.23	
	V	44.5	0.26	
IR18 221.7 km	14A V	-	-	
	T	-	-	
	R	-	-	
	HTL V	5.91	0.27	34.5
	T	4.12	0.40	
	R	5.49	0.38	
	19L V	9.62	0.32	
	V	7.36	0.23	
	V	9.23	0.27	
IR19 285.9 km	14A V	-	-	
	T	-	-	
	R	-	-	
	HTL V	1.42	0.36	42.8
	T	1.57	0.46	
	R	1.47	0.40	
	19L V	1.50	0.35	
	V	1.75	0.34	
	V	2.05	0.37	

V, T, R = Vertical, transverse, and radial components of motion.

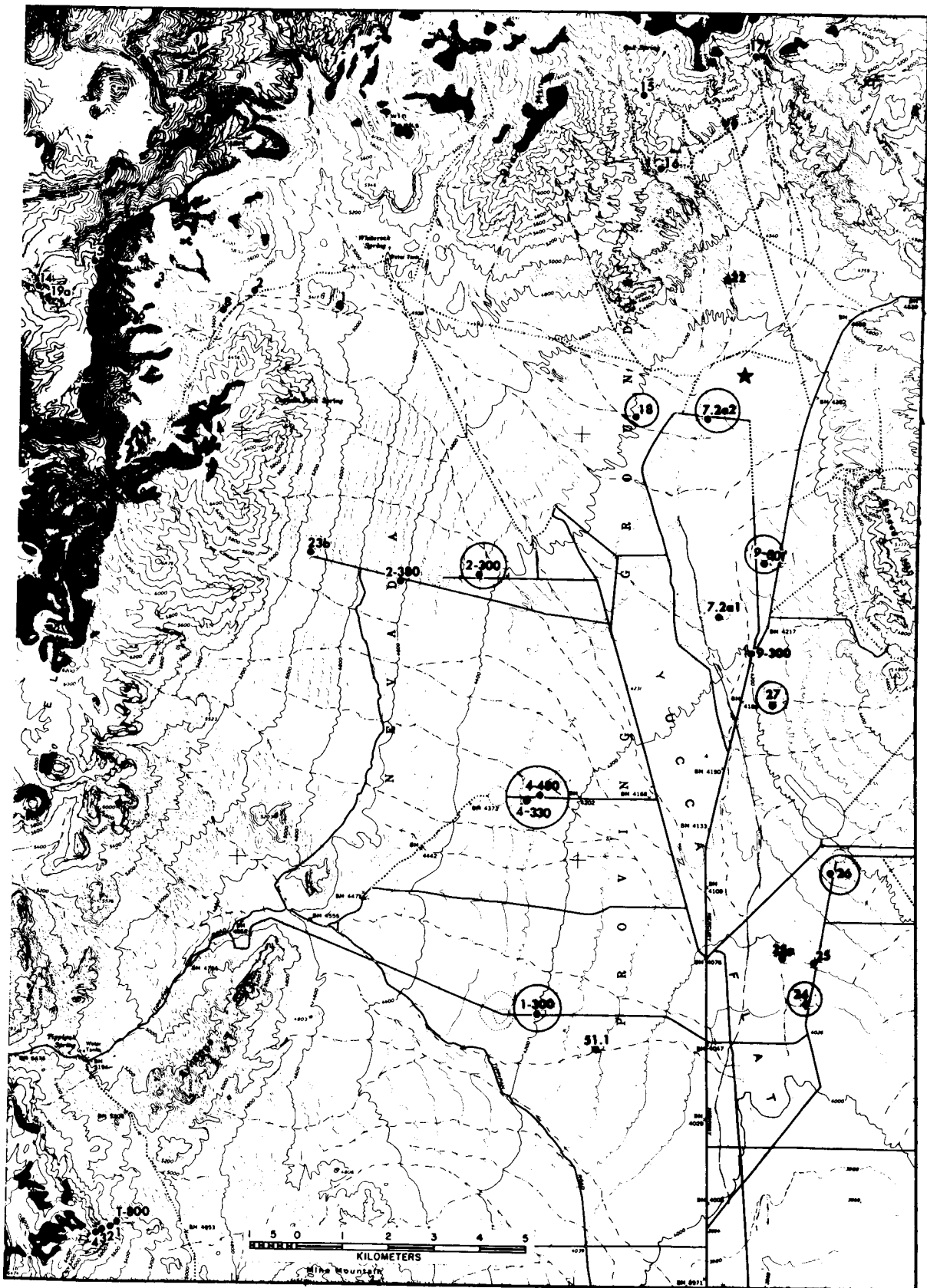
14A, HTL, 19L = Geophone systems as described in text.

NOTE: Signals were not discernible above background on high frequency 14A system.

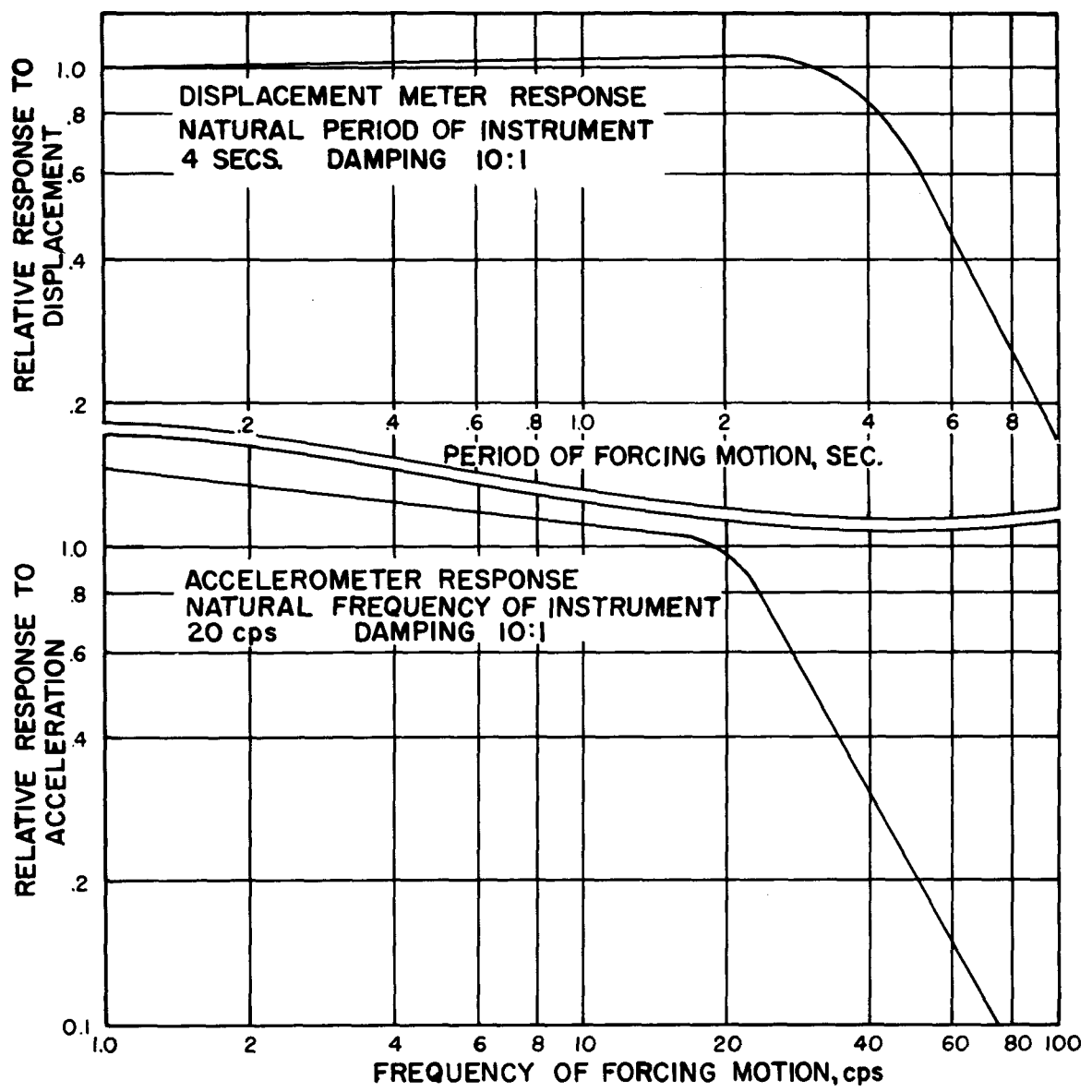
## REFERENCES

1. Berg, J.W., Jr., and K.L. Cook; "Energies, Magnitudes, and Amplitudes of Seismic Waves from Quarry Blasts at Promontory and Lakeside, Utah"; July 1961; *Bulletin of the Seismological Society of America*, Vol. 51, No. 3.
2. Carder, D.S., W.K. Cloud, L.M. Murphy, and J. Hershberger; "Operation PLUMBOB, Surface Motions from an Underground Explosion," WT-1530, AEC Category, Physics and Mathematics; June 1958.
3. Carder, D.S., L.M. Murphy, T.H. Pearce, W.V. Mickey, and W.K. Cloud; "Operation HARDTACK Phase II, Surface Motions from Underground Explosions," WT-1741; March 1961.
4. Carder, D.S., W.V. Mickey, L.M. Murphy, W.K. Cloud, J.N. Jordan, and D.W. Gordon; "Project GNOME, Seismic Waves from an Underground Explosion in a Salt Bed," AEC PNE-110P, April 1962.
5. Gutenberg, B. and C.F. Richter; "Earthquake Magnitude, Intensity, Energy, and Acceleration"; *Bulletin of the Seismological Society of America*, Vol. 46, pp.105-145, April 1956.
6. Hershberger, John; "A Comparison of Earthquake Accelerations With Intensity Ratings," *Bulletin of the Seismological Society of America*, Vol. 46, No. 4, October 1956.
7. Howell, B.F., Jr., and D. Budenstein; "Energy Distribution in Explosion-Generated Seismic Pulses," January 1955; *Geophysics*, Vol. XX, No. 1.
8. Kelley, John S.; "Moving Earth and Rock with a Nuclear Device"; *Science AAAS*, Vol. 138, October 1962.
9. Mickey, W.V.; "Operation PLOWSHARE, Project SCOOTER, Surface Motion from a Cratering Shot in Desert Alluvium"; U.S. Coast and Geodetic Survey, Interagency Report, 1961.
10. Mickey, W.V. and T.H. Pearce; "Project DANNYBOY, Seismic Effects from a Nuclear Cratering Experiment in Basalt"; DASA, POIR-1813 (ITR-1813), September 1962.
11. Mickey, W.V. and T.H. Pearce; "Operation NOUGAT, Strong Motion Measurements, Project 1.4"; DASA, VUP-2301, October 1962.

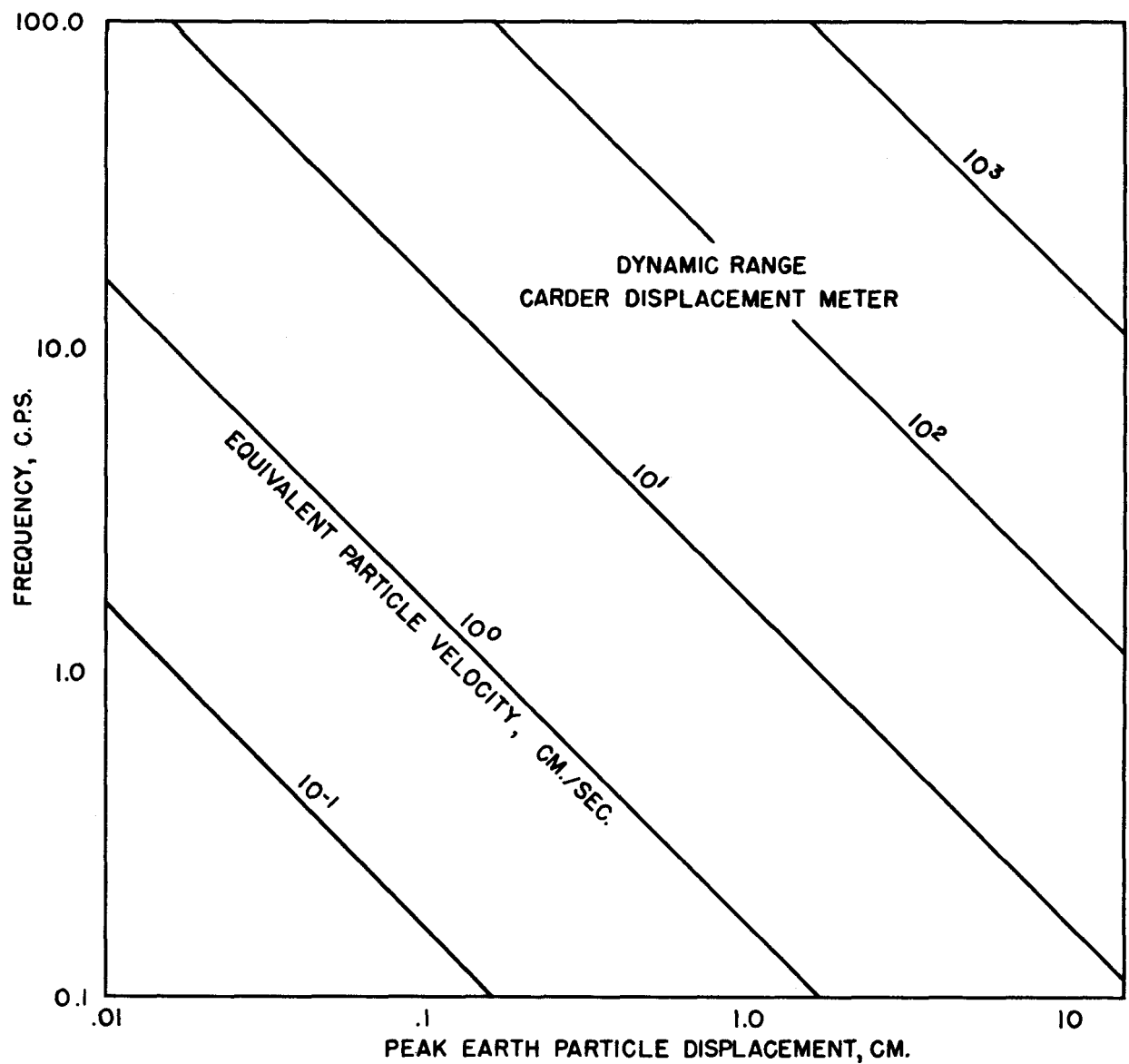
12. Mickey, W.V.; "Operation NOUGAT, Project 8.1, Intermediate Range Seismic Measurements," AFTAC; December 1962.
13. Passechnik, I.P., S.D. Kogan, D.D. Sultanov, and V.I. Tsilbul'skiy; "The Results of Seismic Observations Made During Underground Nuclear and TNT Blasts"; Transactions of the Institute of Physics of the Earth, No. 15 (182), Moskva, USSR Academy of Sciences; 1960.
14. Richter, C.F.; "Elementary Seismology"; W.H. Freeman and Company, 1958.



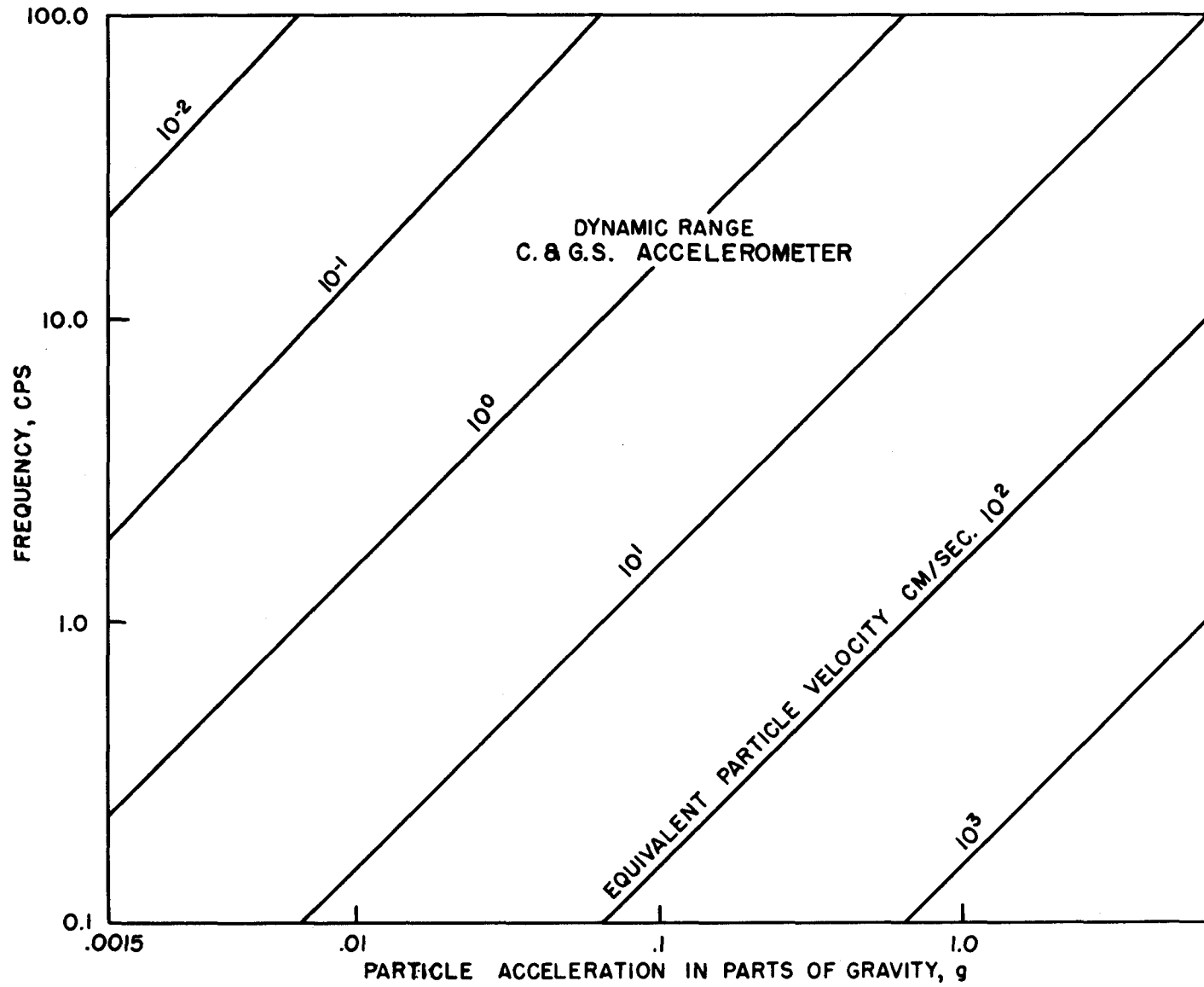
## 2.1 Strong-motion seismograph station



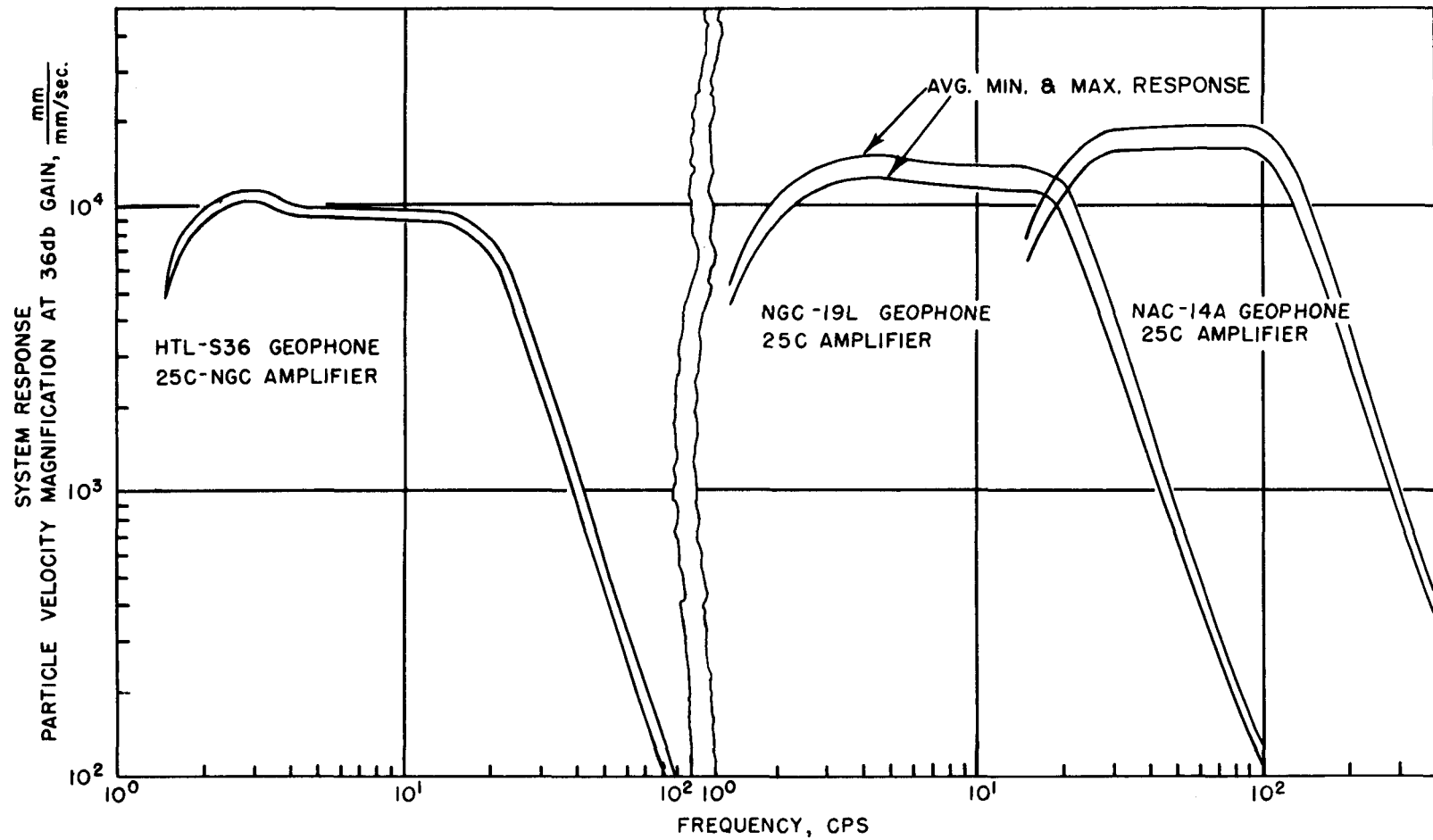
2.2 Response curves for a typical Carder Displacement Meter and an accelerometer



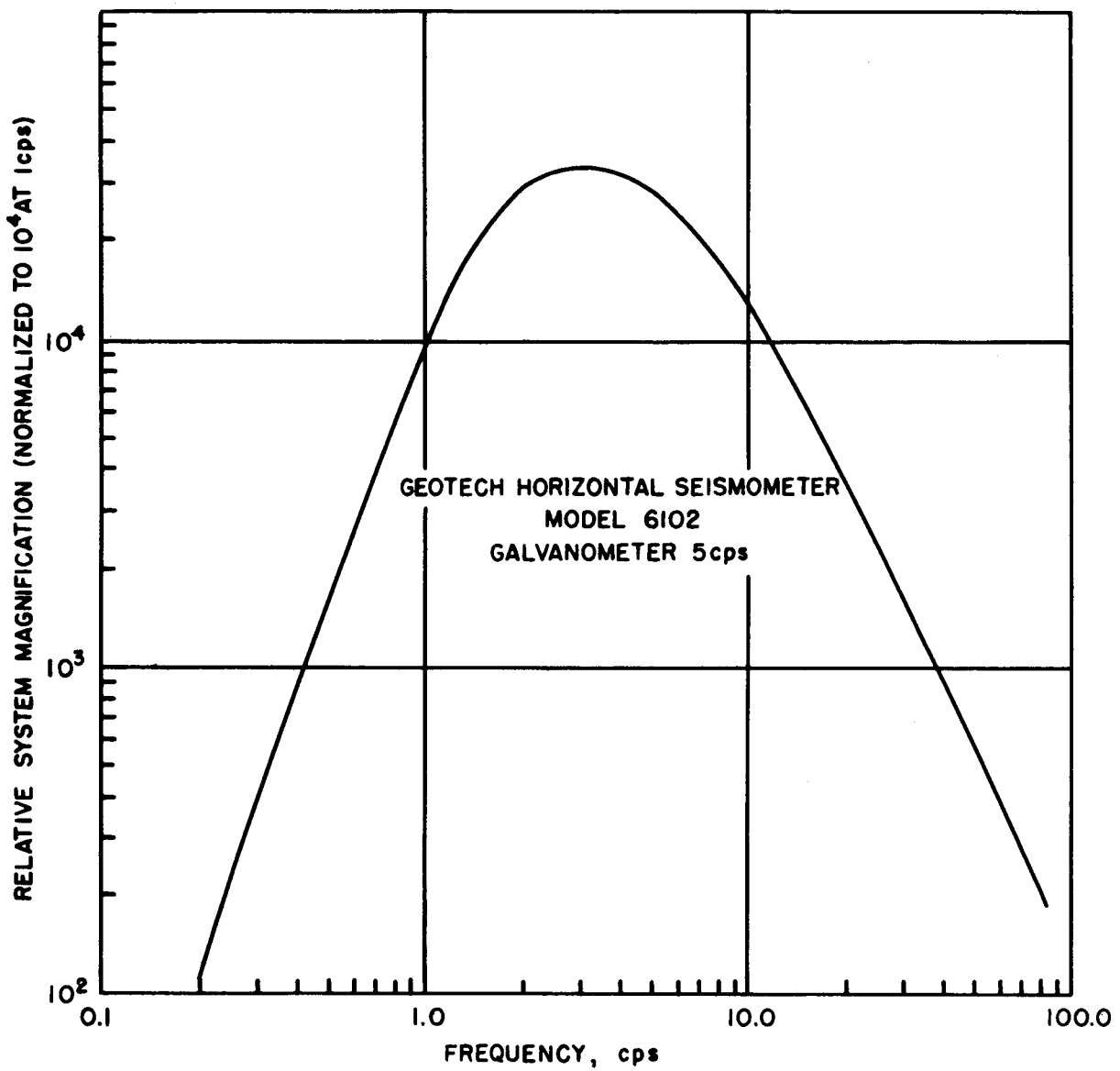
2.3 Dynamic range of displacement meter



2.4 Dynamic range of accelerometer



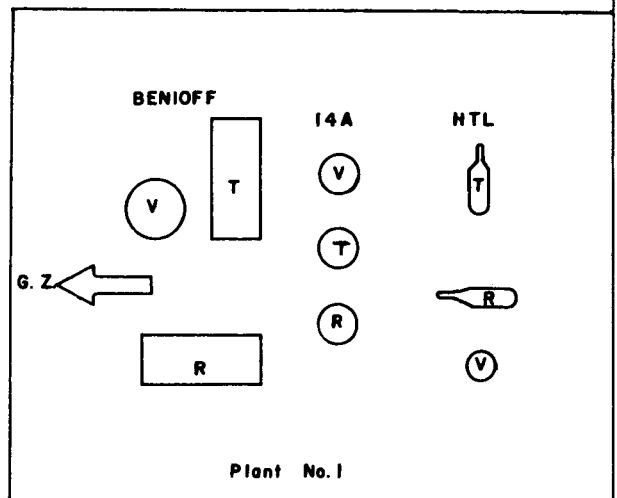
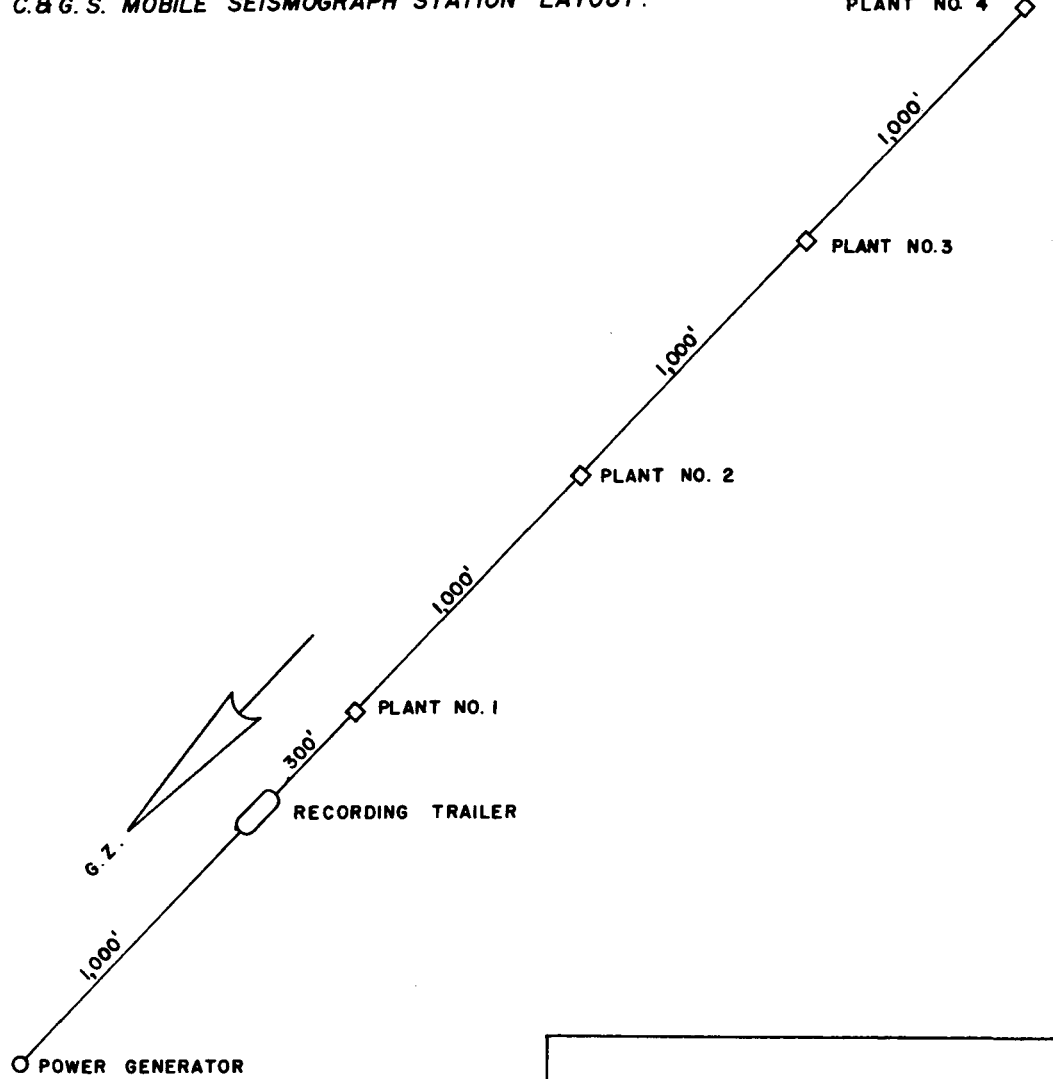
2.5 System response for HTL, 14A, and 19L geophones



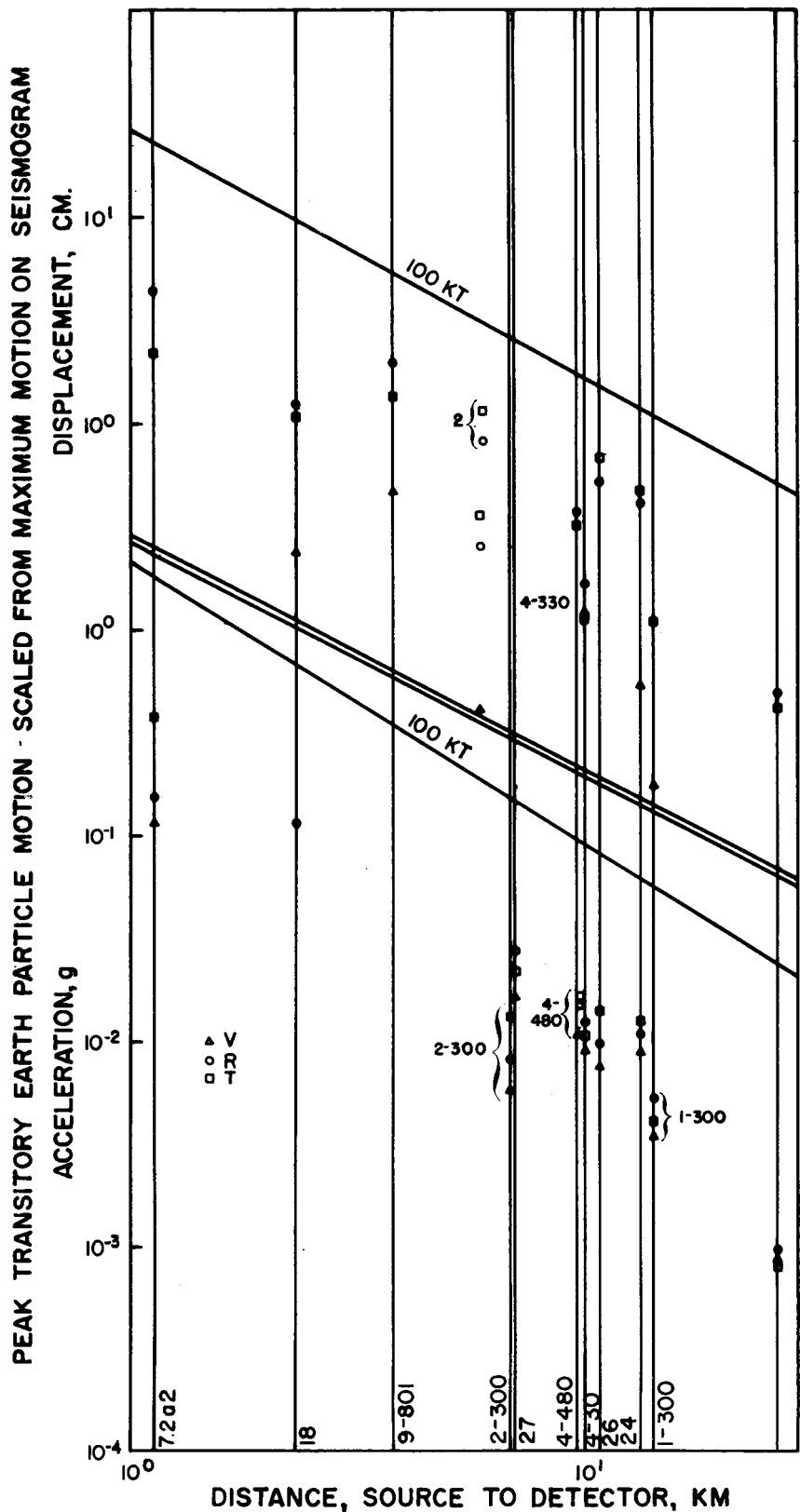
2.6 System response for Model 6102 seismometer

C. & G. S. MOBILE SEISMOGRAPH STATION LAYOUT.

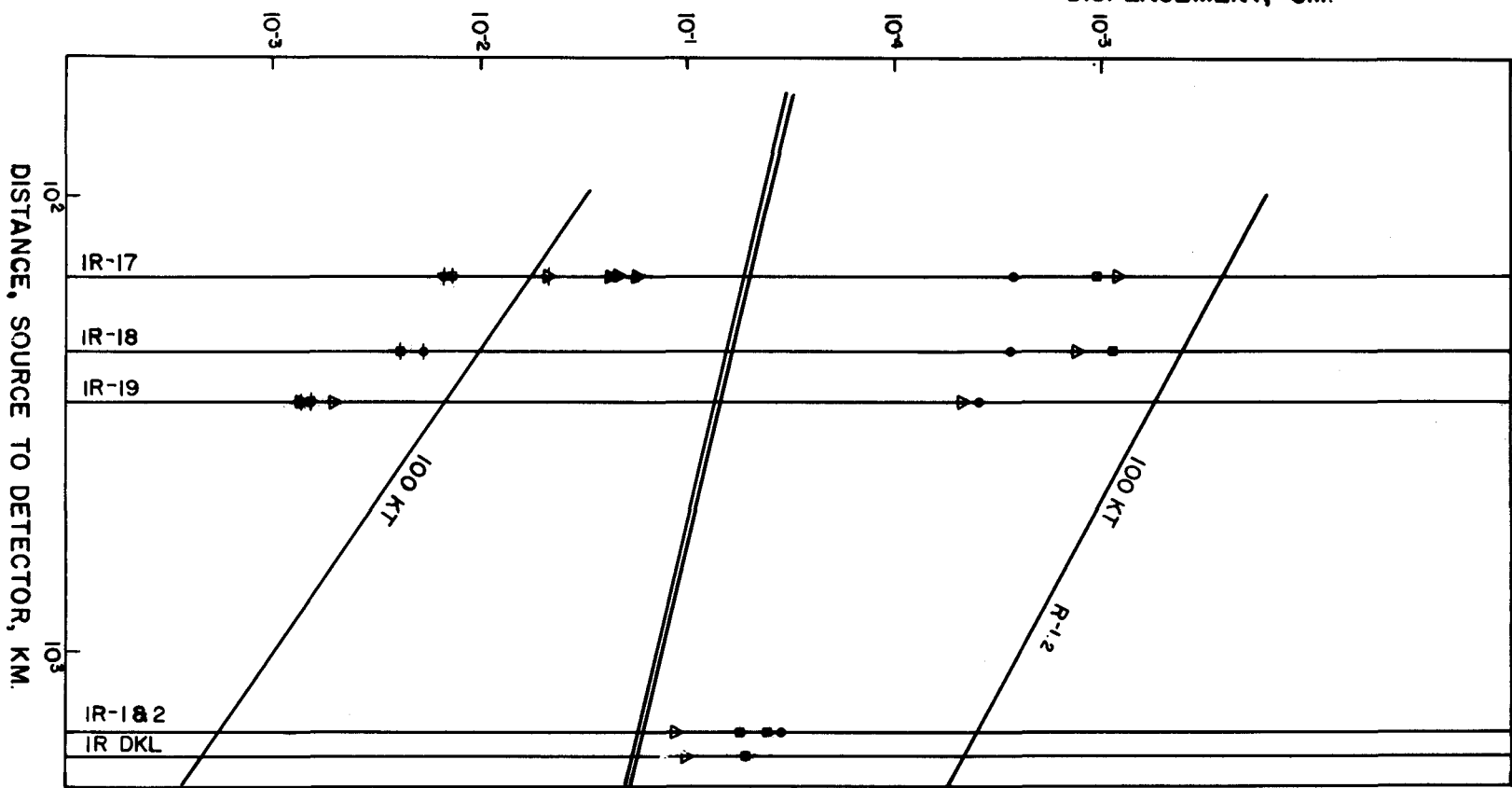
PLANT NO. 4



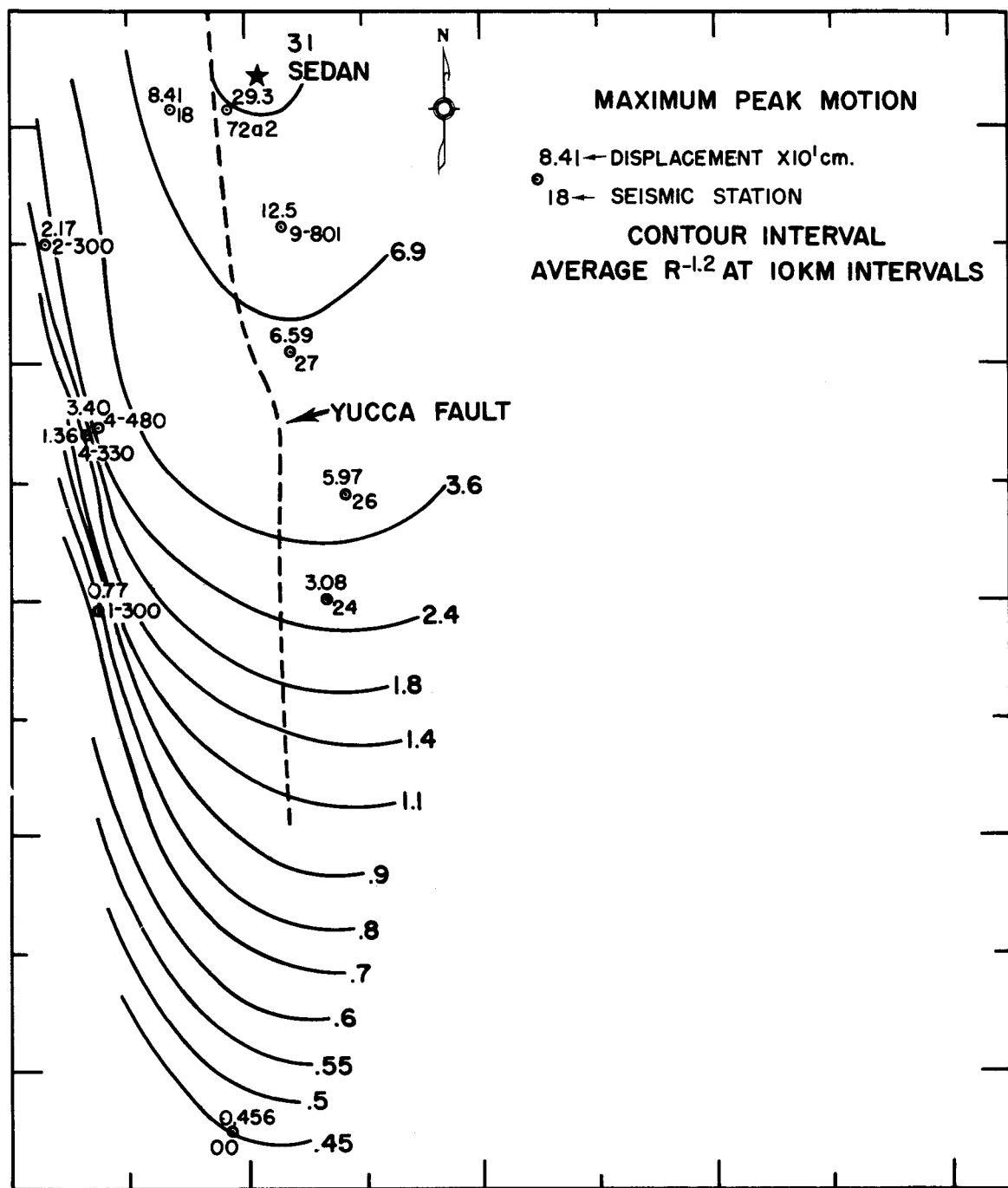
2.7 Mobile station seismometer layout



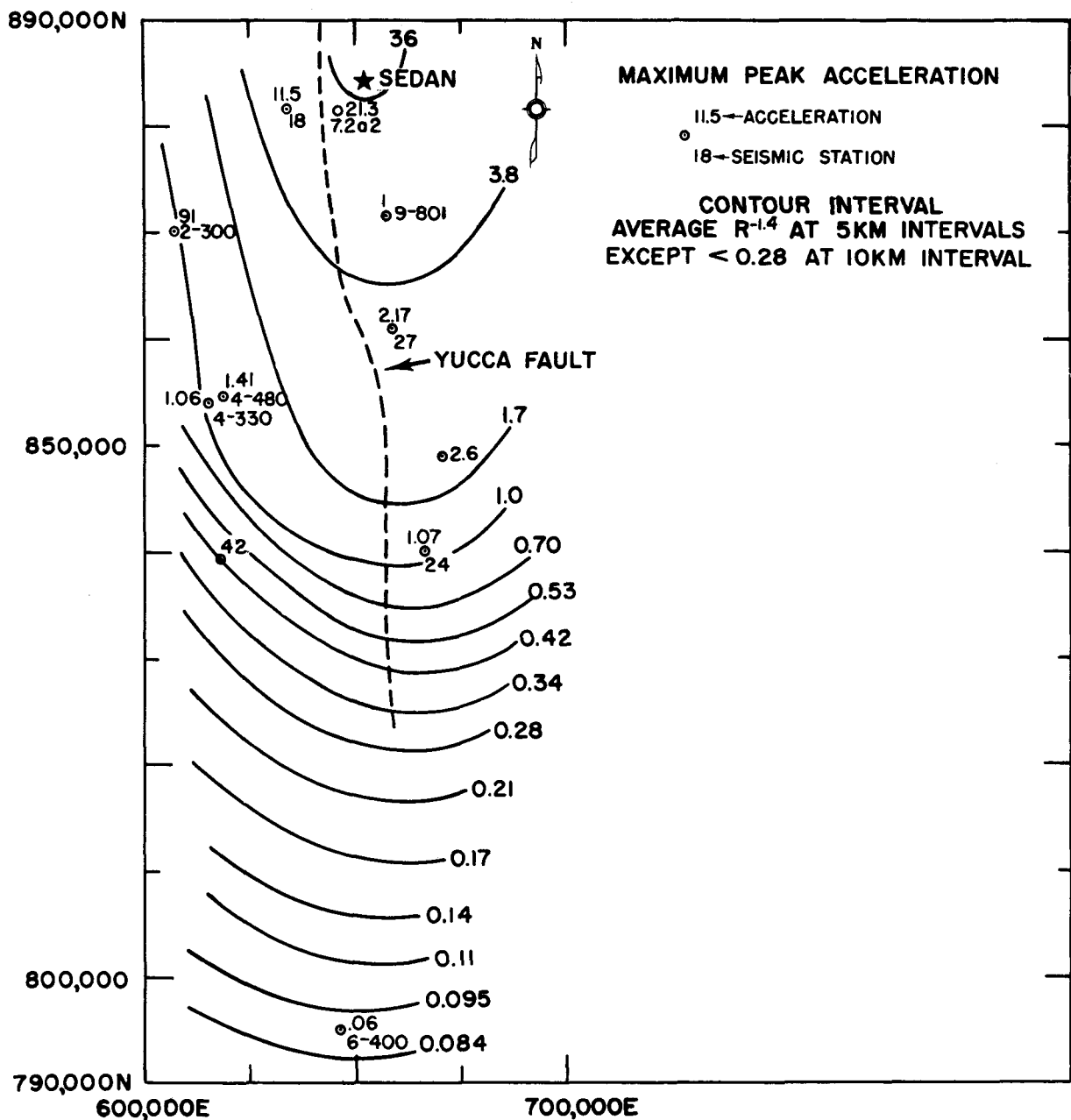
3.1 Observed particle accelerations and displacements from strong-motion stations. The solid line represents the prediction function



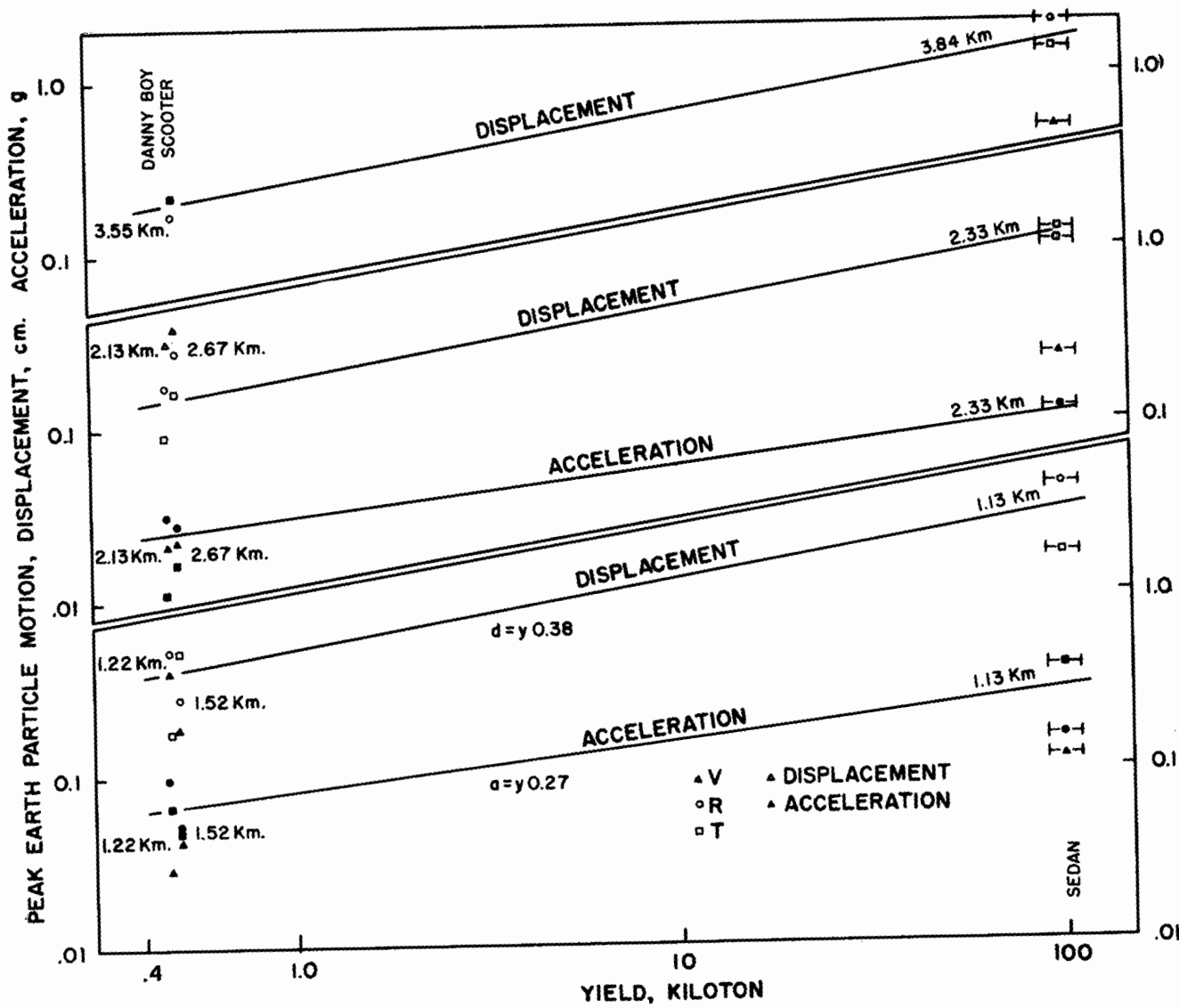
### 3.2 Observed particle velocities and displacements from the intermediate range mobile seismograph stations



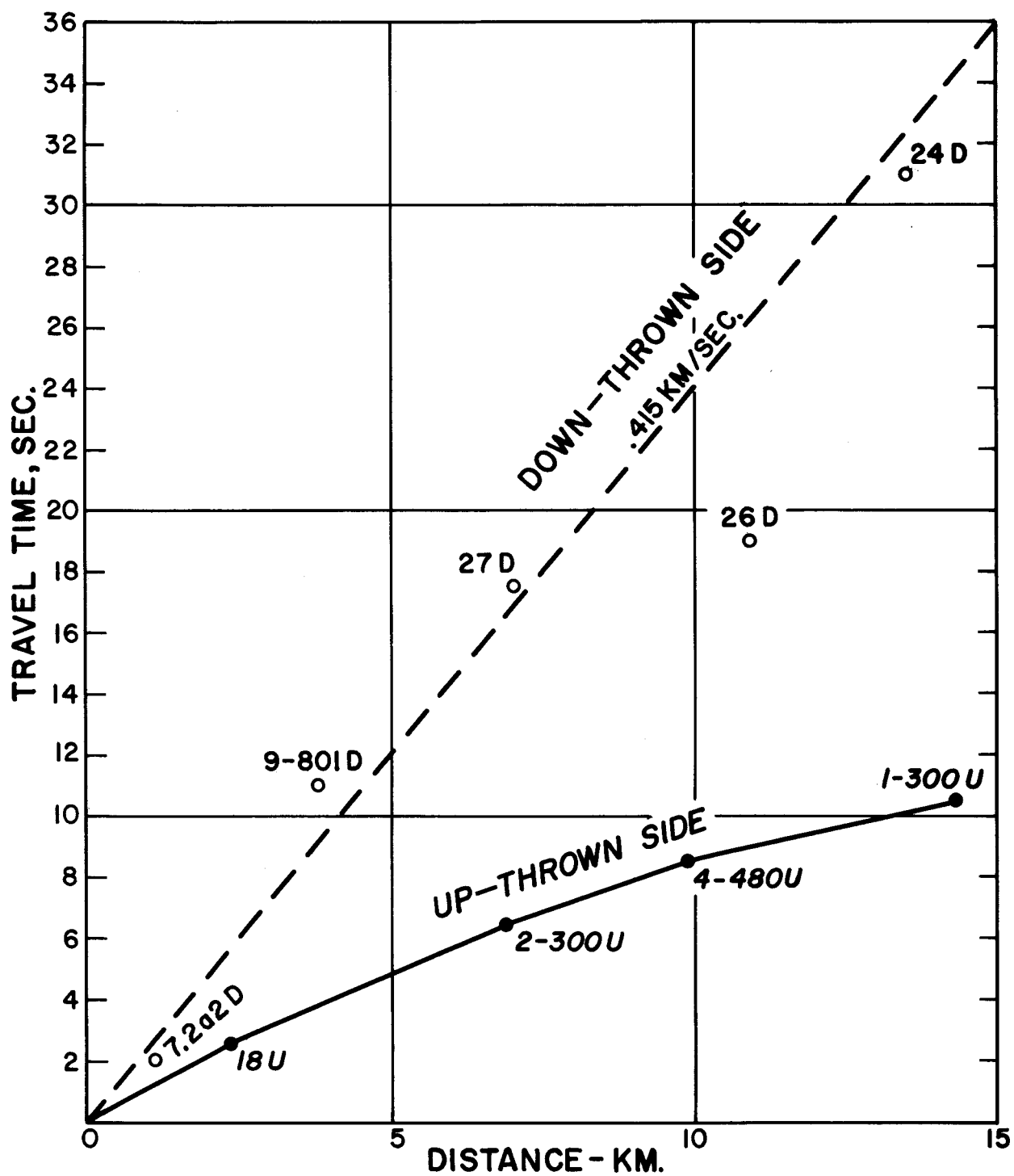
3.3 SEDAN and seismograph station locations contoured from observed displacements



3.4 SEDAN and seismograph station locations contoured from observed accelerations

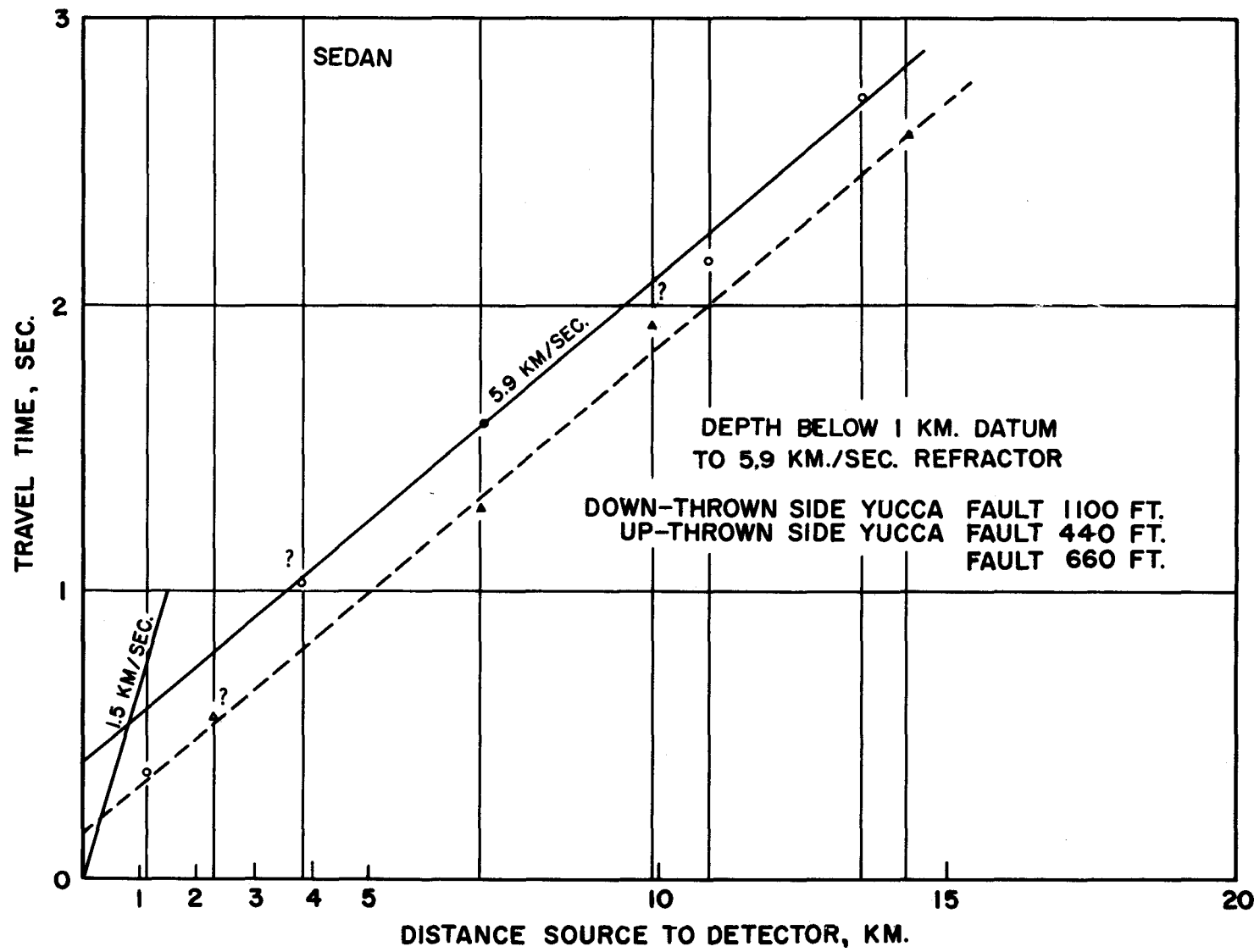


3.5 Surface earth motion versus yields for SCOOTER, DANNYBOY, and SEDAN

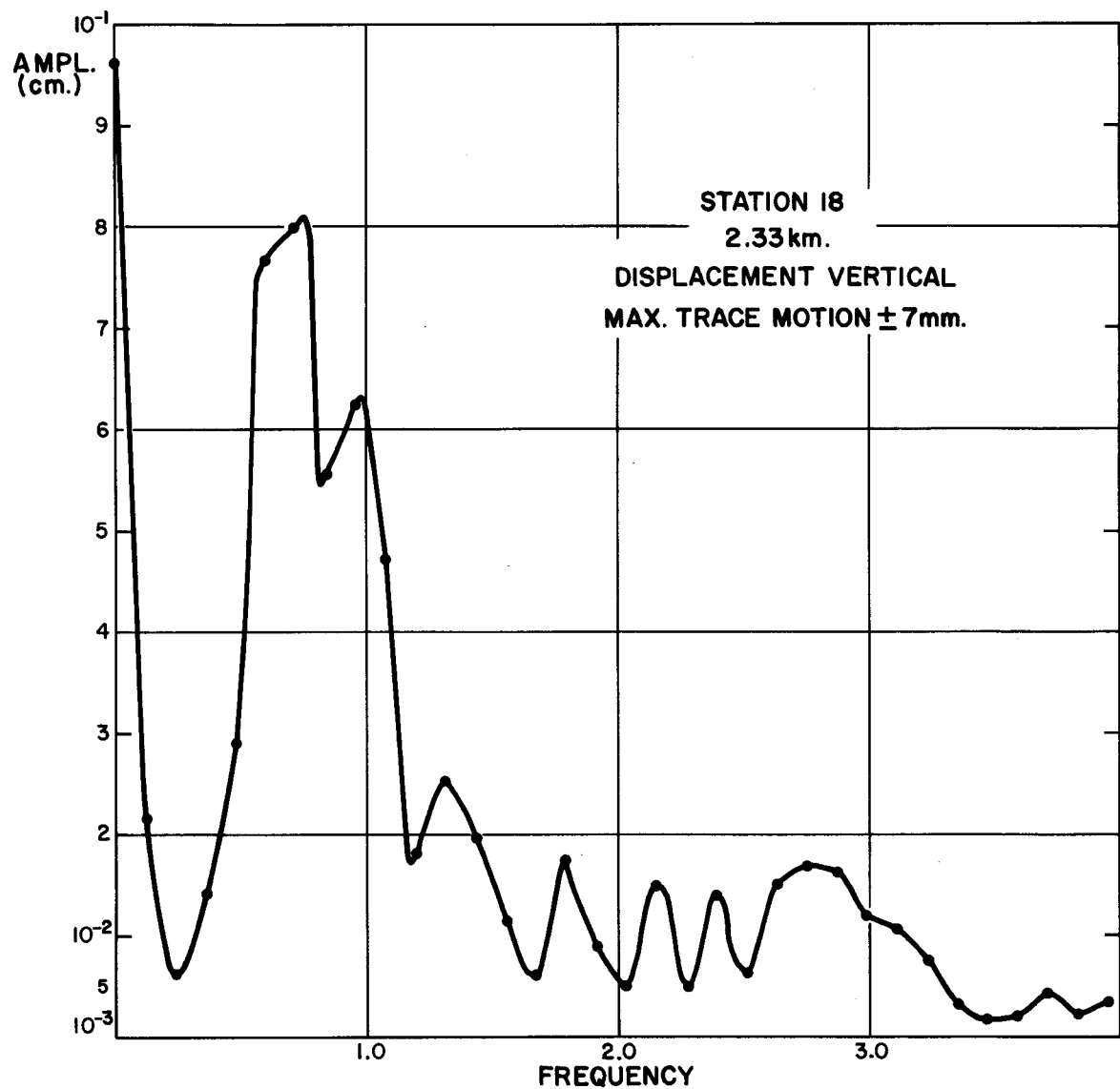


3.6 Travel time - distance plot of maximum earth motion

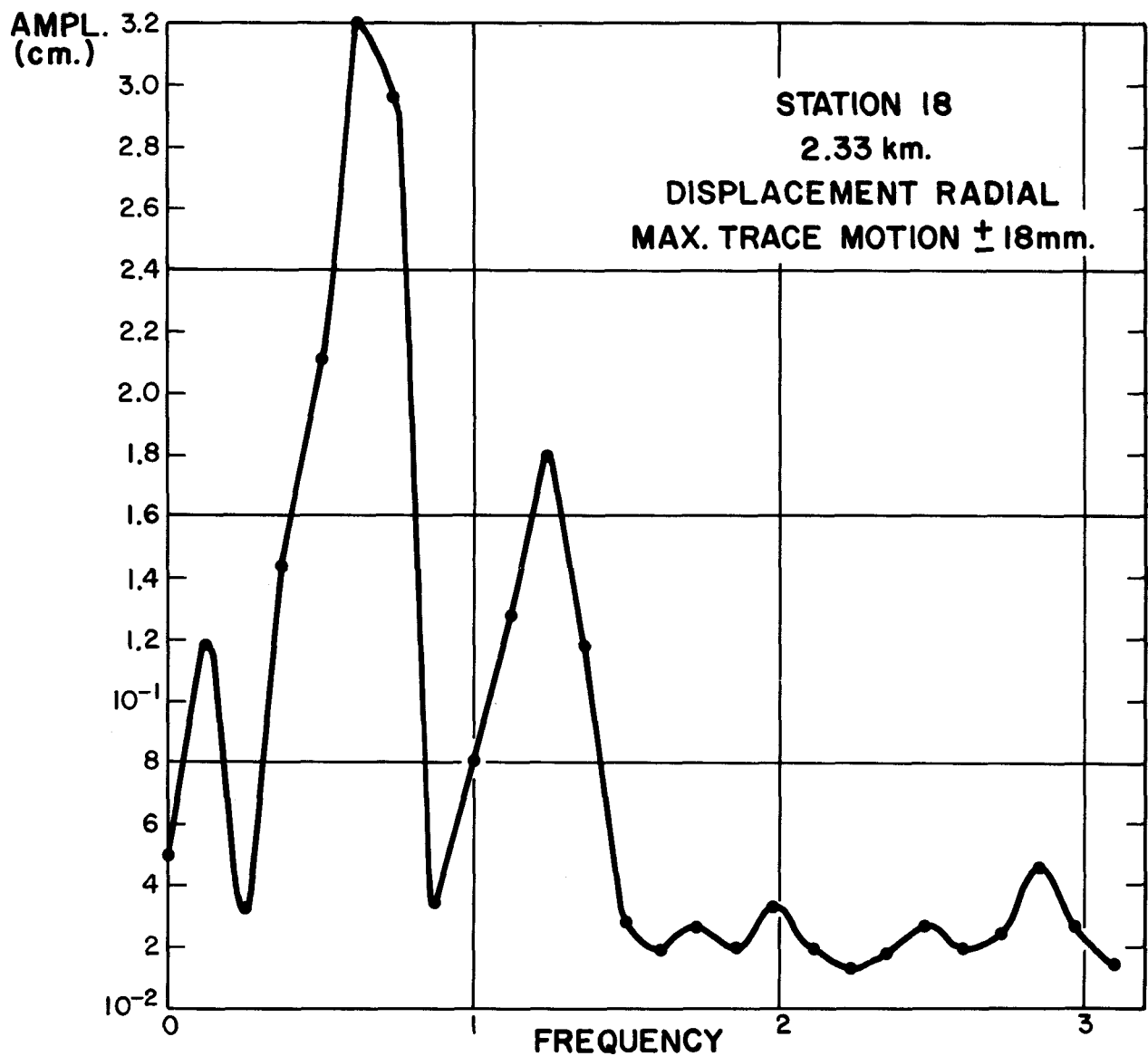
87



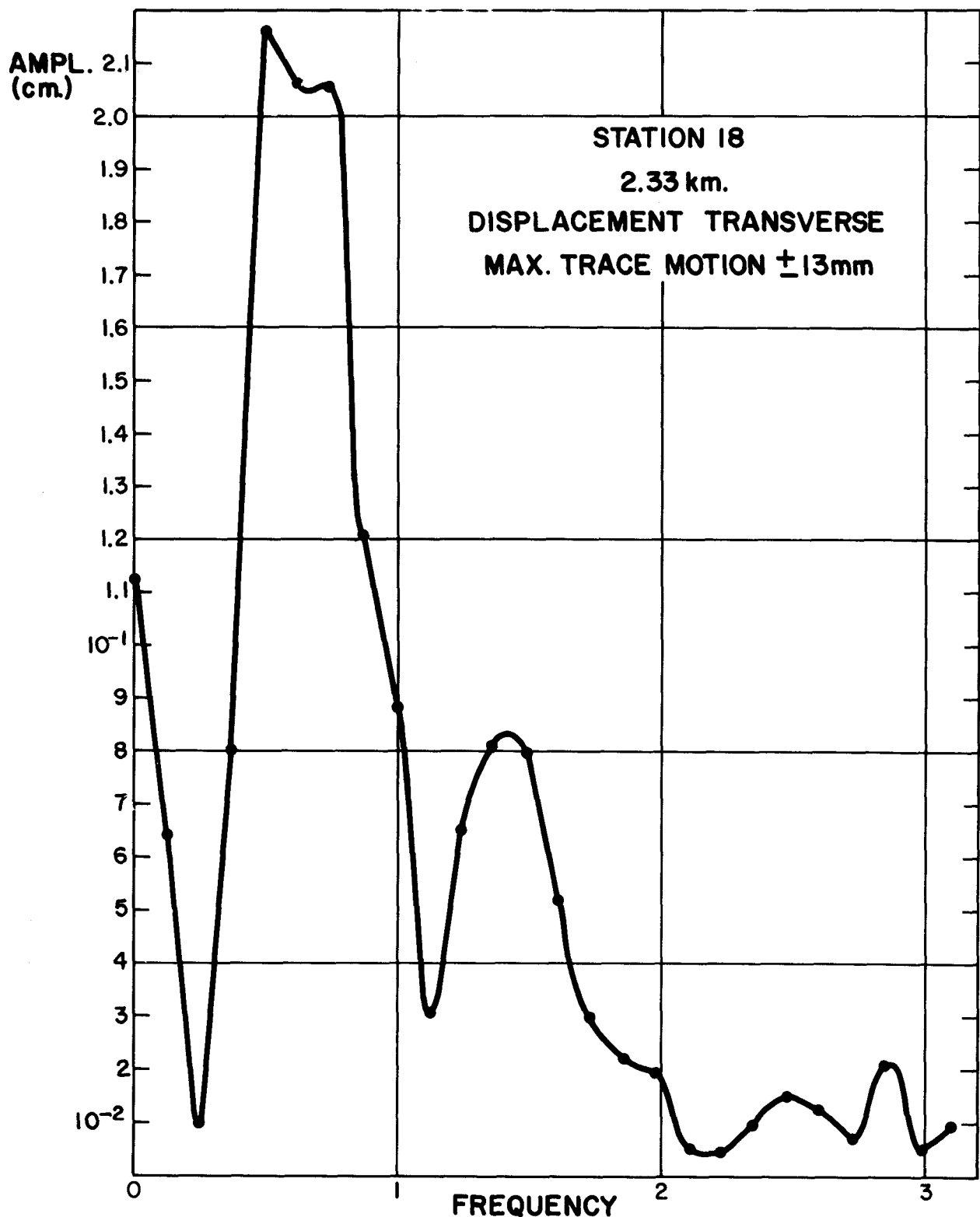
3.7 Travel time - distance plot of first arrivals of seismic energy



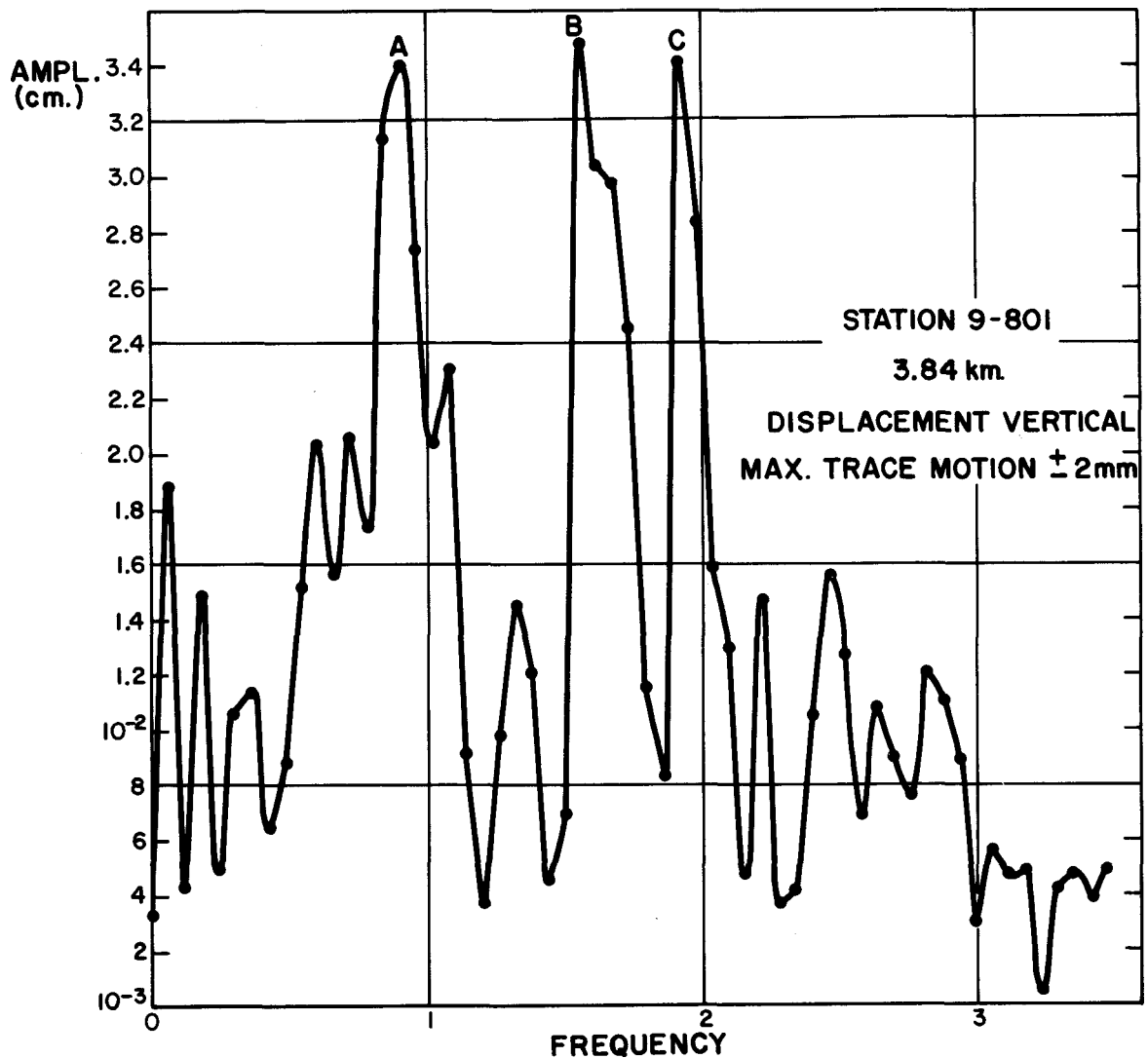
3.8 Frequency versus amplitude from vertical component of displacement at Station 18



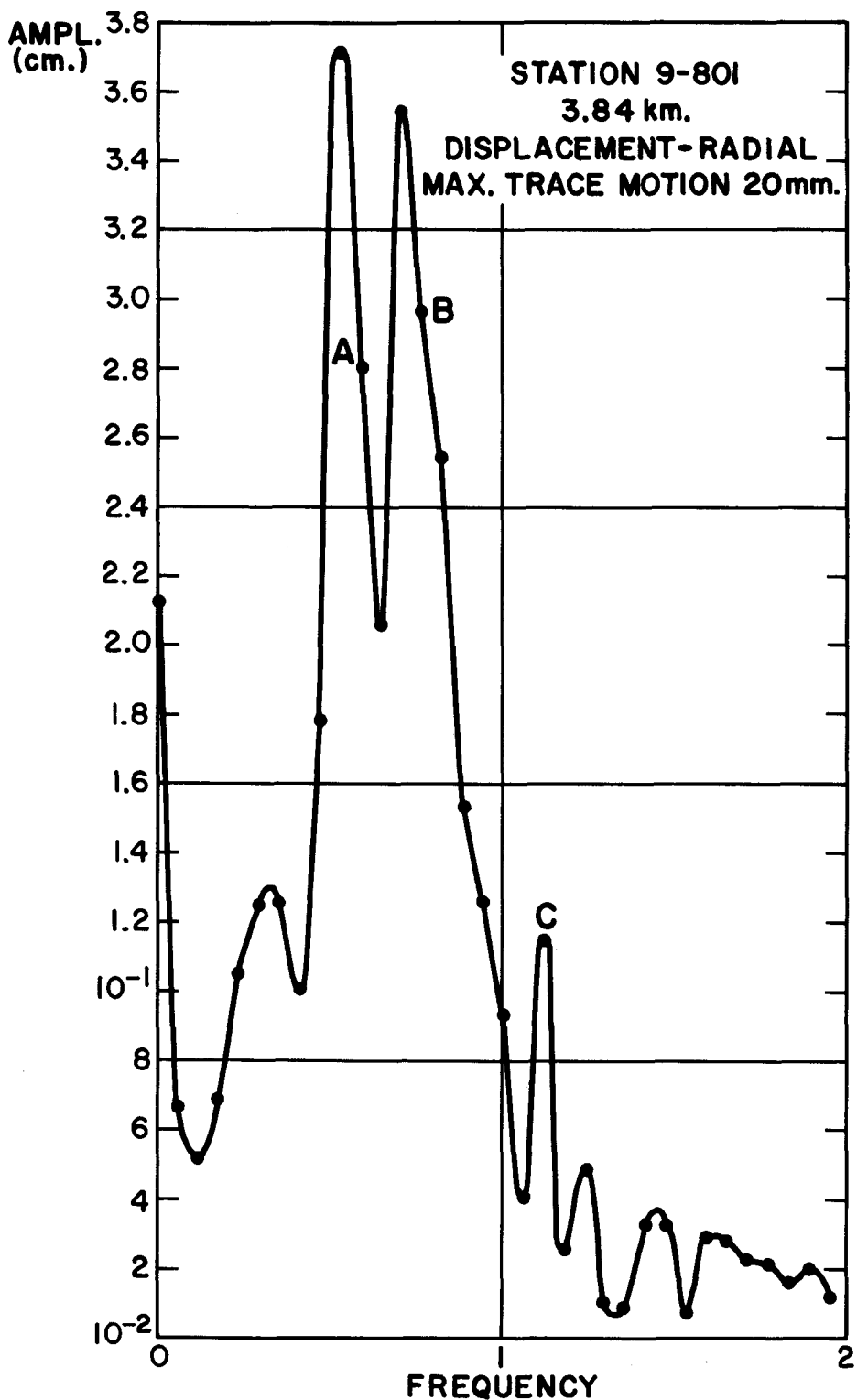
### 3.9 Frequency versus amplitude from radial component of displacement at Station 18



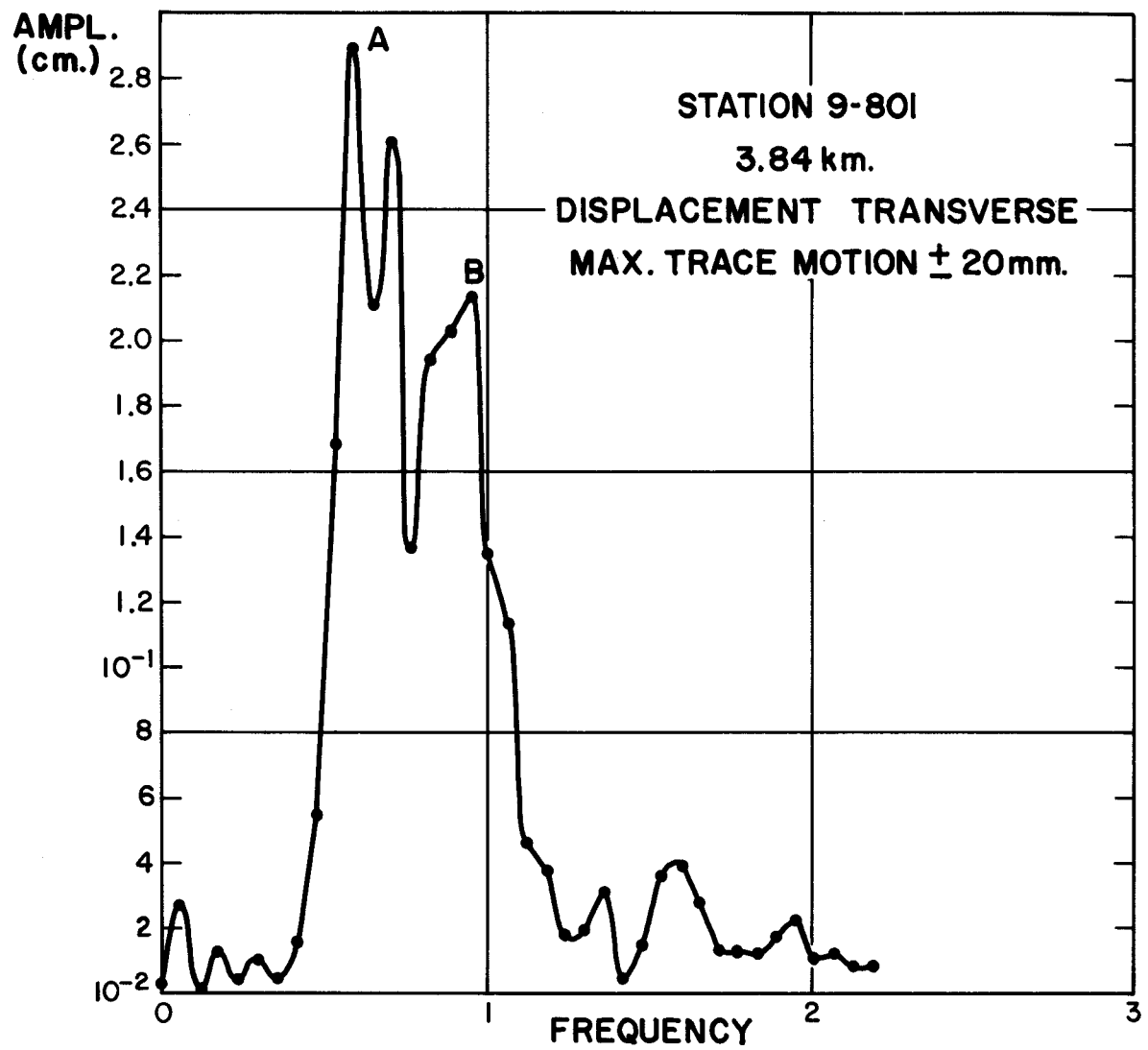
3.10 Frequency versus amplitude from transverse component of displacement at Station 18



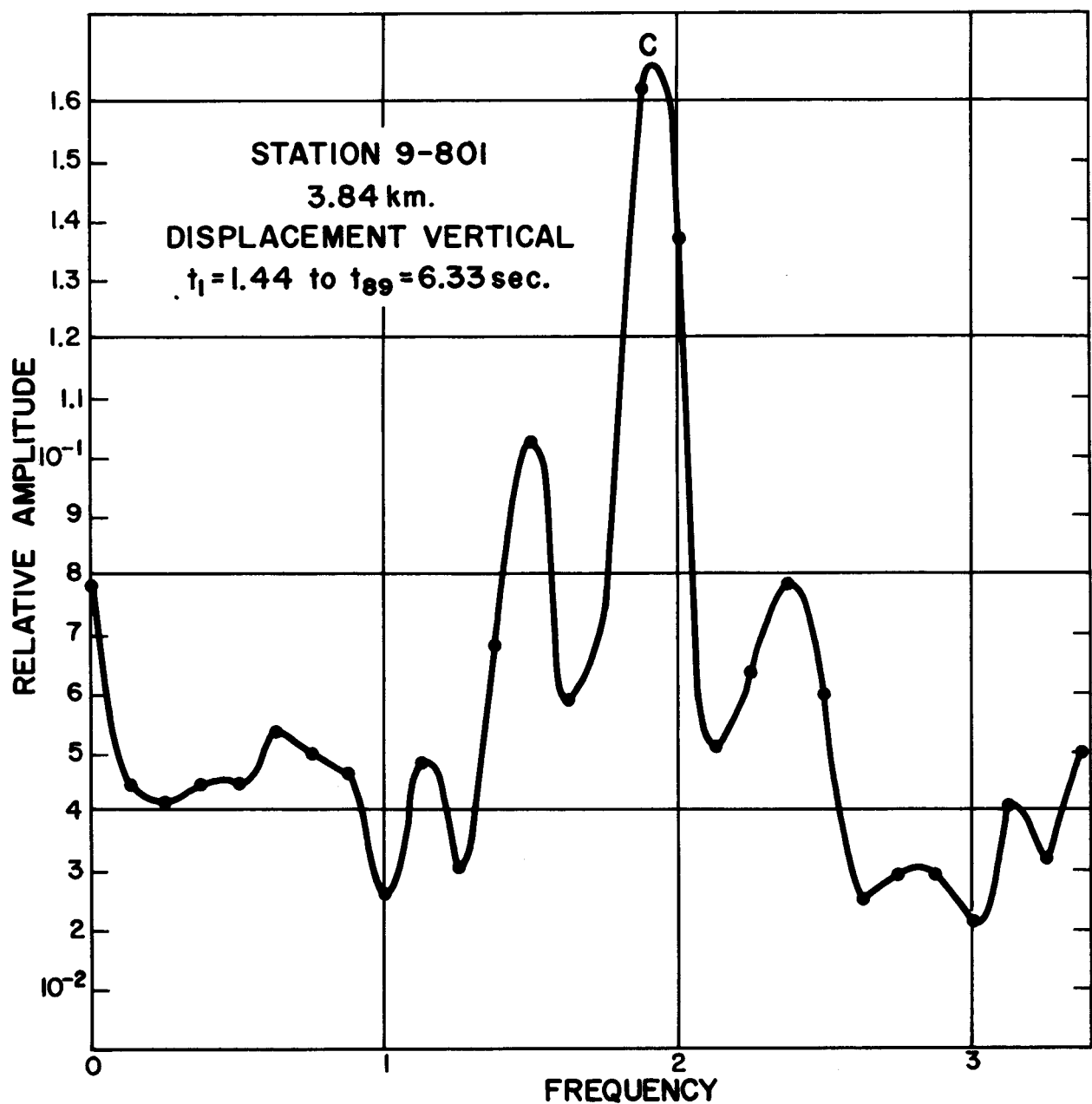
3.11 Frequency versus amplitude from vertical component of displacement at Station 9-801



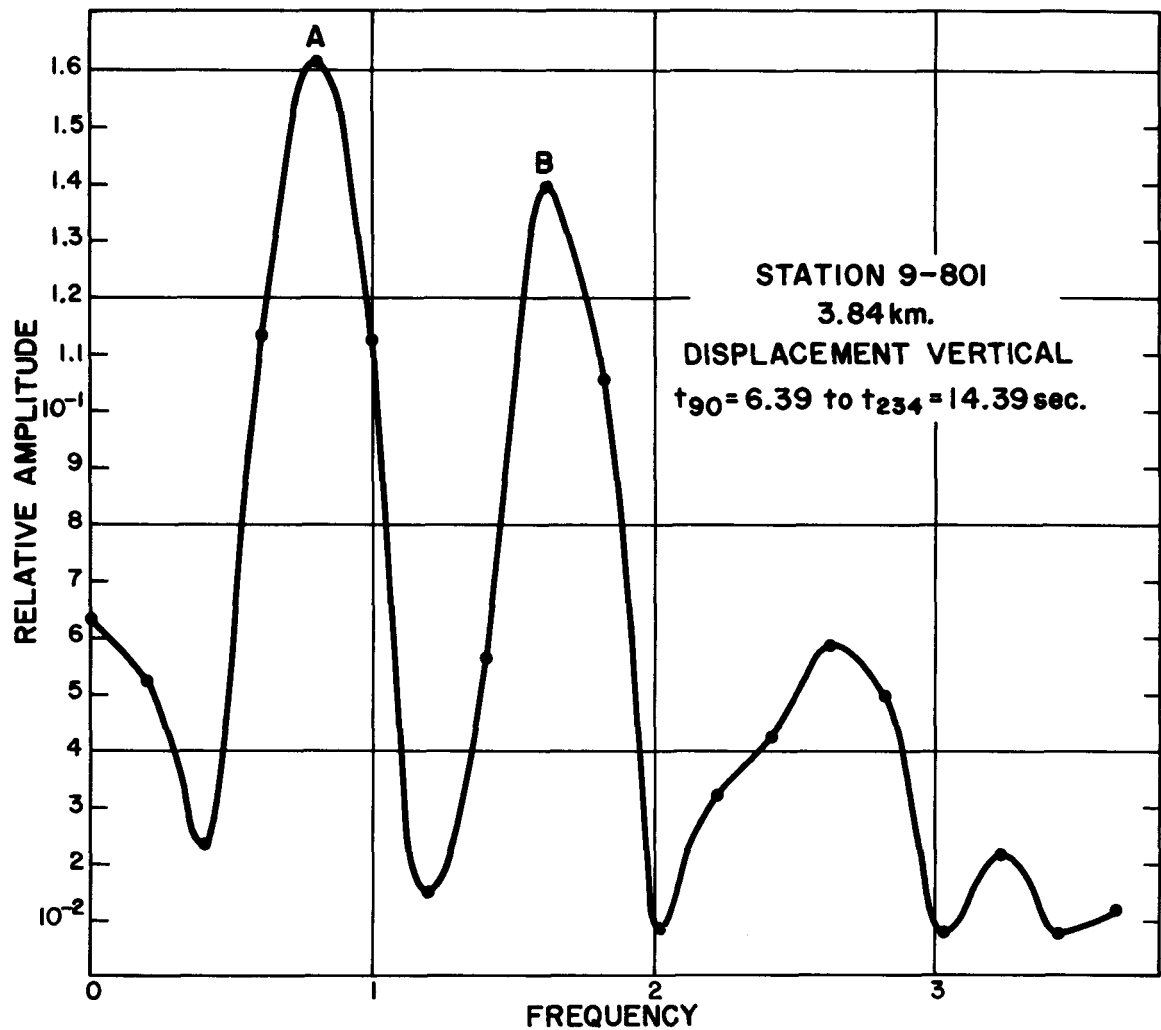
Frequency versus amplitude from radial component of displacement  
at Station 9-801



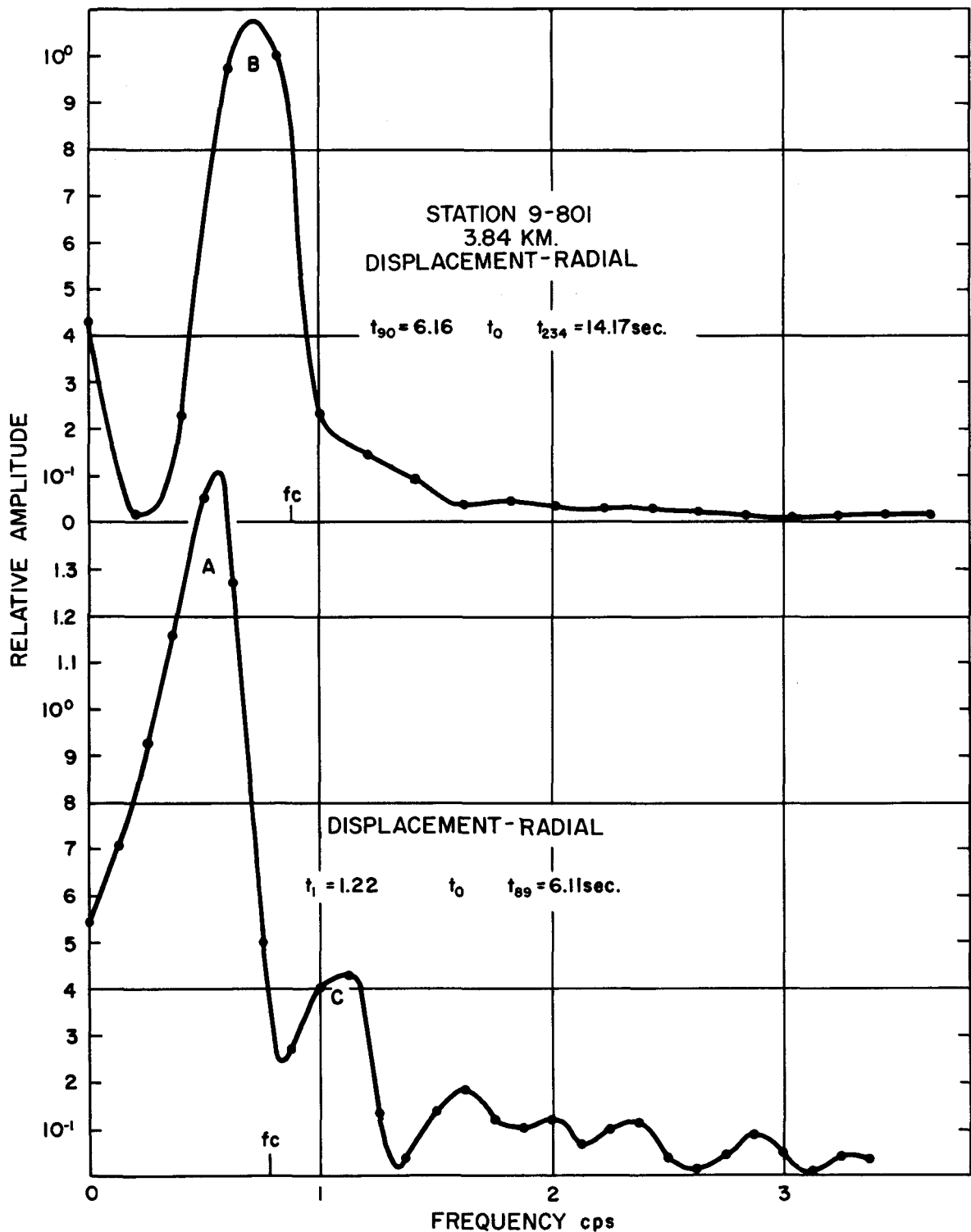
3.13 Frequency versus amplitude from transverse component of displacement at Station 9-801



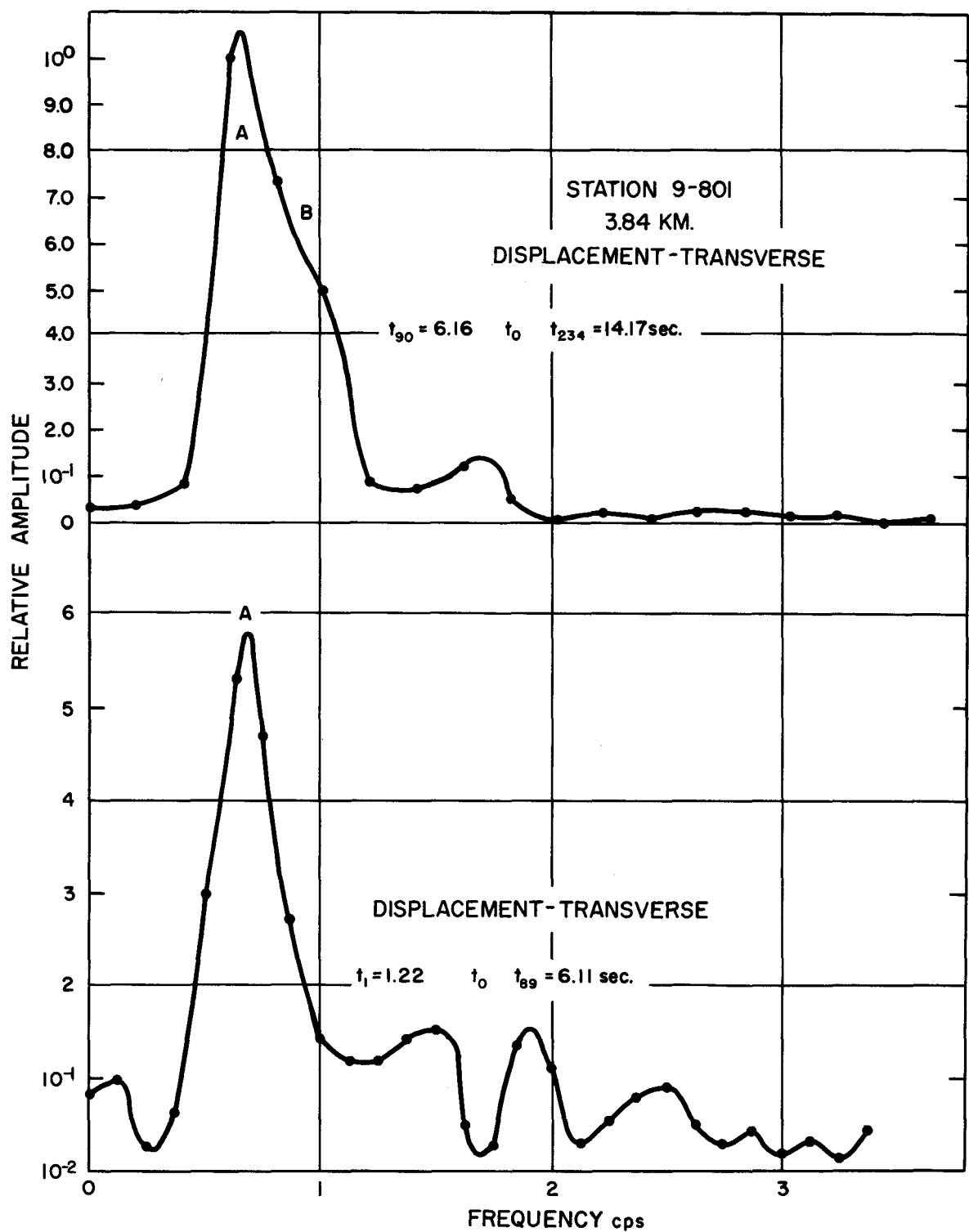
3.14 Frequency versus amplitude for first 89 digital values of figure 3.11 representing real time of 1.44 to 6.33 seconds



3.15 Frequency versus amplitude for digital values 90 through 234 of figure 3.11.  
This is a continuation of figure 3.14 representing real time interval  
of 6.33 through 14.39 seconds



3.16 Frequency versus amplitude for digital values 1 through 89 and 90 through 234 of figure 3.12. This represents two real time segments of 1.22 to 6.11 seconds and 6.16 to 14.17 seconds



3.17 Frequency versus amplitude for digital values 1 through 89 and 90 through 234 of figure 3.13. This represents two real time segments of 1.22 to 6.11 seconds and 6.16 to 14.17 seconds

TECHNICAL REPORTS SCHEDULED FOR ISSUANCE  
BY AGENCIES PARTICIPATING IN PROJECT SEDAN

AEC REPORTS

<u>AGENCY</u>	<u>PNE NO.</u>	<u>SUBJECT OR TITLE</u>
USPHS	200F	Off-Site Radiation Safety
USWB	201F	Analysis of Weather and Surface Radiation Data
SC	202F	Long Range Blast Propagation
REECO	203F	On-Site Rad-Safe
AEC/USBM	204F	Structural Survey of Private Mining Operations
FAA	205F	Airspace Closure
SC	211F	Close-In Air Blast From a Nuclear Event in NTS Desert Alluvium
LRL-N	212P	Scientific Photo
LRL	214P	Fallout Studies
LRL	215F	Structure Response
LRL	216P	Crater Measurements
Boeing	217P	Ejecta Studies
LRL	218P	Radioactive Pellets
USGS	219F	Hydrologic Effects, Distance Coefficients
USGS	221P	Infiltration Rates Pre and Post Shot
UCLA	224P	Influences of a Cratering Device on Close-In Populations of Lizards
UCLA	225P Pt. I and II	Fallout Characteristics

**TECHNICAL REPORTS SCHEDULED FOR ISSUANCE  
BY AGENCIES PARTICIPATING IN PROJECT SEDAN**

<u>AGENCY</u>	<u>PNE NO.</u>	<u>SUBJECT OR TITLE</u>
BYU	226P	Close-In Effects of a Subsurface Nuclear Detonation on Small Mammals and Selected Invertebrates
UCLA	228P	Ecological Effects
RLR	231F	Rad-Chem Analysis
RLR	232P	Yield Measurements
EGG	233P	Timing and Firing
WES	234P	Stability of Cratered Slopes
RLR	235F	Seismic Velocity Studies

**DOD REPORTS**

<u>AGENCY</u>	<u>PNE NO.</u>	<u>SUBJECT OR TITLE</u>
USC-GS	213P	"Seismic Effects From a High Yield Nuclear Cratering Experiment in Desert Alluvium"
NRDL	229P	"Some Radiochemical and Physical Measurements of Debris from an Underground Nuclear Explosion"
NRDL	230P	Naval Aerial Photographic Analysis

### ABBREVIATIONS FOR TECHNICAL AGENCIES

STL	Space Technology Laboratories, Inc., Redondo Beach, Calif.
SC	Sandia Corporation, Sandia Base, Albuquerque, New Mexico
USC&GS	U. S. Coast and Geodetic Survey, San Francisco, California
LRL	Lawrence Radiation Laboratory, Livermore, California
LRL-N	Lawrence Radiation Laboratory, Mercury, Nevada
Boeing	The Boeing Company, Aero-Space Division, Seattle 24, Washington
USGS	Geological Survey, Denver, Colorado, Menlo Park, Calif., and Vicksburg, Mississippi
WES	USA Corps of Engineers, Waterways Experiment Station, Jackson, Mississippi
EGG	Edgerton, Germeshausen, and Grier, Inc., Las Vegas, Nevada, Santa Barbara, Calif., and Boston, Massachusetts
BYU	Brigham Young University, Provo, Utah
UCLA	UCLA School of Medicine, Dept. of Biophysics and Nuclear Medicine, Los Angeles, Calif.
NRDL	Naval Radiological Defense Laboratory, Hunters Point, Calif.
USPHS	U. S. Public Health Service, Las Vegas, Nevada
USWB	U. S. Weather Bureau, Las Vegas, Nevada
USBM	U. S. Bureau of Mines, Washington, D. C.
FAA	Federal Aviation Agency, Salt Lake City, Utah
REECO	Reynolds Electrical and Engineering Co., Las Vegas, Nevada

**SUPPLEMENTARY DOD DISTRIBUTION FOR PROJECT SEDAN**

<u>PNE NO.</u>	<u>DIST. CAT.</u>	<u>PNE NO.</u>	<u>DIST. CAT.</u>	<u>PNE NO.</u>	<u>DIST. CAT.</u>
200	26, 28	214	26	226	42
201	2, 26	215	32	228	42
202	12	216	14	229	26, 22
203	28	217	14	230	100
204	32	218	12, 14	231	22
205	2	219	14	232	4
211	12	221	14	233	2
212	92, 100	224	42	234	14
213	12, 14	225	26	235	14

In addition, one copy of reports 201, 202, 203, 211, 214, 215, 216, 217, 218, 221, 225, 229, 230, 232, 234, and 235 to each of the following:

The Rand Corp.  
1700 Main St.,  
Santa Monica, California

Attn: Mr. H. Brode

U. of Illinois,  
Civil Engineering Hall  
Urbana, Illinois

Attn: Dr. N. Newmark

Stanford Research Institute  
Menlo Park, California

Attn: Dr. Vaile

E. H. Plessset Associates  
1281 Westwood Blvd.,  
Los Angeles 24, California

Attn: Mr. M. Peter

Mitre Corp.  
Bedford, Massachusetts

General American Transportation Corp.  
Mechanics Research Div.  
7501 N. Natchez Ave.,  
Niles 48, Illinois

Attn: Mr. T. Morrison; Dr. Schiffman

Dr. Whitman  
Massachusetts Institute of Technology  
Cambridge, Massachusetts